European Journal of Neuroscience

Methodological Considerations for Studying Neural Oscillations

|---|---|
Manuscript ID	EJN-2021-01-28100(RIC)
Manuscript Type:	Special Issue Technical Spotlight
Date Submitted by the Author:	18-Jan-2021
Complete List of Authors:	Donoghue, Thomas; University of California San Diego, Cognitive Science Schaworonkow, Natalie; University of California San Diego, Cognitive Science Voytek, Bradley; University of California San Diego, Cognitive Science
Key Words:	neural field data, digital signal processing, electrophysiology, time series analysis, spectral analysis

SCHOLARONE™
Manuscripts

1 **Title**
2 Methodological Considerations for Studying Neural Oscillations
3 *short title: analysis of neural oscillations*
4
5 **Authors**

6 Thomas Donoghue[1], Natalie Schaworonkow[1], & Bradley Voytek[1, 2, 3,4]
7
8 *Affiliations*
9 [1]Department of Cognitive Science, University of California, San Diego
10 [2]Neurosciences Graduate Program, University of California, San Diego
11 [3]Halıcıoğlu Data Science Institute, University of California, San Diego
12 [4]Kavli Institute for Brain and Mind, University of California, San Diego
13
14 *Corresponding Author*
15 Thomas Donoghue: tdonoghue.research@gmail.com
16
17 *Contributions*
18 All authors contributed to designing the study. T.D and N.S did the analyses and created the figures. All
19 authors contributed to writing and editing the paper.
20
21 *ORCIDs*
22 Donoghue   0000-0001-5911-0472
23 Schaworonkow   0000-0002-2103-1178
24 Voytek   0000-0003-1640-2525
25

26 Disclosures
27

41 **Materials Descriptions & Availability Statements**

42

43 **Project Repository**

44

45 This project is also made openly available through an online project repository in which the code
46 and data are made available, with step-by-step guides through the analyses.
47

48   Project Repository: https://github.com/voytekresearch/OscillationMethods

49

50 **Datasets**

51

52 This project uses simulated data. Code to recreate the exact simulations used is included in the
53 project repository.

54

55 **Software**

56

57 Code used and written for this project was written in the Python programming language (>=v3.7).
58 All the code used within this project is deposited in the project repository and is made openly
59 available and licensed for reuse.

60

61 This project uses the following Python packages for simulating and analyzing neural data:

62

63   neurodsp   https://neurodsp-tools.github.io/
64   fooof   https://fooof-tools.github.io/
65   bycycle   https://bycycle-tools.github.io/

66

67 In addition, third party Python toolboxes including mne, numpy, scipy, matplotlib, and seaborn
68 were used in this project.

69

Abstract

Neural oscillations are ubiquitous across recording methodologies and species, broadly associated with cognitive tasks, and amenable to computational modeling that investigates neural circuit generating mechanisms and mesoscale dynamics. Because of this, neural oscillations may offer an exciting potential opportunity for linking theory, physiology, and mechanisms of cognition. However, despite their prevalence, there are many concerns—new and old—about how our analysis assumptions are violated by known properties of field potential data. For investigations of neural oscillations to be properly interpreted, and ultimately developed into mechanistic theories, it is necessary to carefully consider the underlying assumptions of the methods we employ. Here, we discuss seven methodological considerations for analyzing neural oscillations. The considerations are to 1) verify the presence of oscillations, as they may be absent; 2) validate oscillation band definitions, to address variable peak frequencies; 3) account for concurrent non-oscillatory aperiodic activity, which might otherwise confound measures; measure and account for 4) temporal variability and 5) waveform shape of neural oscillations, which are often bursty and/or nonsinusoidal, potentially leading to spurious results; 6) separate spatially overlapping rhythms, which may interfere with each other; and 7) consider the required signal-to-noise ratio for obtaining reliable estimates. For each topic, we provide relevant examples, demonstrate potential errors of interpretation, and offer suggestions to address these issues. We primarily focus on univariate measures, such as power and phase estimates, though we discuss how these issues can propagate to multivariate measures. These considerations and recommendations offer a helpful guide for measuring and interpreting neural oscillations.

Keywords

neural field data, digital signal processing, electrophysiology, time series analysis, spectral analysis

Abbreviations

EEG: electroencephalography; MEG: magnetoencephalography; SNR: signal-to-noise ratio

Introduction

Recordings of electrical or magnetic fields in the brain, collectively referred to as neural field recordings, are commonly used for investigating links between physiology and behavior, cognition, and disease. A striking feature of such recordings is the prominent, structured, rhythmic activity, termed neural oscillations (Buzsáki & Draguhn, 2004), that stands out in the otherwise seemingly chaotic activity of the brain. Neural oscillations have been a feature of interest since the early days of electrical brain recordings (Brazier, 1958), and are widely observed, being ubiquitously present across species (Buzsáki et al., 2013). Physiologically, field potential recordings largely reflect the aggregate postsynaptic and transmembrane currents of thousands to millions of neurons (Buzsáki et al., 2012), with neural oscillations thought to relate to population synchrony (Wang, 2010). As such, neural oscillations potentially offer insight into the coordination of neural activity at the mesoscopic level. Accordingly, theories of the functions of oscillations argue that they facilitate dynamic temporal and spatial organization of neural activity (Fries, 2005; VanRullen, 2016; Varela et al., 2001; Voytek & Knight, 2015). Correspondingly, disruptions of oscillations have been widely linked to neurological and psychiatric disease, and have been explored as potential biomarkers of disease status, drug efficacy, and other clinical indicators (Başar, 2013; Buzsáki & Watson, 2012; Newson & Thiagarajan, 2019).

Reflecting this broad interest, thousands of investigations conducted across many decades have reported associations between oscillations and just about every aspect of behavior and cognition that can be operationalized (Başar et al., 2001; Lopes da Silva, 2013; Mazaheri et al., 2018). As neural oscillations appear at many different temporal scales (Buzsáki et al., 2013), investigations often focus on predefined canonical frequency band ranges that are thought to capture distinct oscillations. For example, sleep researchers often study delta (1-4 Hz), memory researchers theta (4-8 Hz), visual researchers alpha (8-12 Hz), and cognitive and motor researchers beta (13-30 Hz) frequency bands. In doing so, research in neural oscillations spans across different recording modalities (Buzsáki et al., 2012)—including both non-invasive and invasive methods—and across different brain regions (Frauscher et al., 2018; Mahjoory et al., 2020).

While oscillations provide an exciting possibility to link cognition and disease to theory and physiology, there are often inconsistent reports regarding which oscillations are modulated by which conditions and how. In part, this likely reflects the variety of approaches taken, with limited

132 consistency in terms of experimental design, analysis methods, parameter choices, and
133 theoretical frameworks used across studies. Open challenges include developing more consistent
134 terminology and interpretations (Cohen & Gulbinaite, 2014), and the need for explicitly
135 considering replicability in electrophysiological investigations (Cohen, 2017a). Accordingly, best
136 practice guidelines for research (Pernet et al., 2020; Pesaran et al., 2018) and clinical
137 investigations (Babiloni et al., 2020) have recently been proposed to improve standards of
138 reporting, and therefore reproducibility, for research using neural field recordings.

139

140 As an extension of these general guidelines, here we examine common interpretational
141 considerations in analyzing neural field recordings. Given the advances in both methods
142 development and our understanding of the empirical properties of the data under study, it is
143 critically important to ensure that common analysis methods are appropriately applied, as this is
144 a core requisite for accurate interpretation. There is a large toolkit of analysis methods for studying
145 neural oscillations, across both the spectral and temporal domains, borrowed and adapted from
146 the field of digital signal processing. These methods are described and compared in other work
147 focused on methodological properties of particular estimation techniques (Bruns, 2004; Gross,
148 2014; van Vugt et al., 2007; Wacker & Witte, 2013).

149

150 Here, we focus more explicitly on properties of neural oscillations, and how these
151 properties relate to commonly applied methods, rather than focus on the methods themselves.
152 We address how common analysis approaches can give rise to results that are easy for
153 researchers to misinterpret, due to the misalignment between methodological or experimental
154 assumptions, and properties of the data. As such, these considerations are not restricted to
155 individual estimators (such as using particular filters, or a particular estimate of power), as they
156 reflect more general properties of signal processing methods and neural data. Importantly, these
157 are not failures of the algorithms per se, which do, mathematically, exactly what they should; the
158 potential pitfalls lay in how we interpret their outputs. If and when there is a misalignment between
159 methodological assumptions and data properties, computed measures can lack validity which can
160 lead to inconsistent results. This in turn impedes us from properly grounding oscillation research
161 in physiology and theory.

162

163 To address these issues, we examine common interpretational considerations in studying
164 neural oscillations, in order to identify and address possible methodological concerns that may
165 lead to interpretation errors. We consider recurring themes based on our developing

166 understanding of neural field data, and how this understanding relates to the application of
167 analysis methods. For example, a common assumption is that neural field data can be quantified
168 as a series of oscillatory signals, often assumed to be stationary. However, in empirical
169 neurophysiological data, oscillations show large variability in their presence and extent across
170 time, as well as across participants and cortical regions (Donoghue, Haller, et al., 2020; Frauscher
171 et al., 2018; Groppe et al., 2013). Even when oscillations are present, they are highly variable
172 (Jones, 2016; Neymotin, Barczak, et al., 2020), waxing and waning in short bursts and including
173 longer, more tonic rhythms, with rapidly changing amplitude, frequency, and phase dynamics that
174 are not easily captured by common analyses and predefined canonical frequency ranges. All of
175 these properties, and more, need to be explicitly considered in order to accurately and reliably
176 measure oscillatory neural activity.

177

178 We organize methodological considerations for analyzing neural oscillations into seven
179 areas, each with example demonstrations (see **Box 1**). The primary focus is on univariate
180 measures of oscillatory power, frequency, and phase, including potential pitfalls and
181 considerations for ensuring accurate measurement and interpretation of these aspects, as well
182 as discussions of how these issues can propagate to multivariate analyses, such as cross-
183 frequency coupling. These demonstrations make use of simulated data, which is created to match
184 known properties of neural field recordings whereby key features of the simulated neural field
185 activity were chosen and manipulated to reflect experimentally observed variations in empirical
186 data. We analyze the simulated data using common spectral and time-domain analysis methods
187 in order to evaluate their performance in relation to the interplay of data properties and method
188 assumptions. Each consideration is then contextualized within the broader literature, and specific
189 practical recommendations are made to help guide the analysis of neural oscillations. The
190 simulated data and analysis methods were created and used from the NeuroDSP module (Cole
191 et al., 2019), with all associated code for recreating and further exploring the illustrations openly
192 available in the project repository (https://github.com/voytekresearch/oscillationmethods).

193

194 # #1 Neural oscillations are not always present

195 *Why this matters*

196   Neural field recordings are characterized not only by oscillatory activity, but also aperiodic
197 '1/f' or '1/f-like' activity, in which signal power decreases exponentially as a function of frequency
198 (Freeman et al., 2003; B. J. He, 2014). This is usually formalized as $1/f^\chi$ where χ represents the
199 decay of power across frequencies. In neural data, χ often ranges between 0 and 4, where a
200 signal with $\chi=0$ is white noise, with equal power across all frequencies, and higher values of χ
201 indicate increasingly 'steeper' spectra. Aperiodic neural activity has been linked to the underlying
202 activity of postsynaptic potentials and is a ubiquitous and sometimes dominant feature of neural
203 field data (Gao et al., 2017; K. J. Miller et al., 2009).

204

205   The fact that aperiodic activity is omnipresent together with the large observable variability
206 of neural oscillations (Donoghue, Haller, et al., 2020; Frauscher et al., 2018; Groppe et al., 2013)
207 requires care in how we measure and interpret band-limited power obtained by spectral analysis.
208 Due to the presence of aperiodic activity, there is always non-zero power at all frequency bands.
209 This means that any spectral measure—including computing a power spectrum, narrowband
210 filtering, and average band-power measures—will always return a numerical value for power for
211 a given frequency band, even if there is no oscillatory activity present. That is, just because there
212 is power in a *frequency band* does not imply that there is an *oscillation* in that same frequency
213 band (Bullock et al., 2003). It is a fallacy to presume that an analysis of a predefined narrowband
214 frequency range necessarily reflects physiological oscillatory activity.

215

216   To introduce how transient and aperiodic signals are represented in the spectral domain,
217 we can consider the Dirac delta, in which a single non-zero value in the time domain is
218 represented by constant power across all frequencies in the frequency domain (Fig. 1A). This
219 illustrates that power in a specific frequency band does not generally correspond to a present
220 oscillation in the time domain. Next, we can consider the 1/f-like aperiodic activity which is
221 common in neural data, for which the power spectrum shows power across all frequencies, with
222 decreasing power for higher frequencies (Fig. 1B). Despite the lack of periodic activity in this
223 simulation, narrowband filtering, which imposes a sinusoidal basis, extracts components that
224 appear to be oscillatory, when filtered into canonical band ranges (Fig. 1C). By comparison,
225 rhythmic signals, such as a pure sinusoid, exhibit as a frequency specific peak in the power

226 spectrum (Fig. 1D). We then simulated neural field recordings as a summation of oscillatory and
227 aperiodic components, resulting in a power spectrum that exhibits a spectral peak exceeding the
228 aperiodic component, reflecting a high amount of band-specific power (Fig. 1E). In this case, the
229 presence of the spectral peak is indicative of oscillatory power. In general, since different signal
230 components can contribute to spectral power across different frequency ranges, power in a
231 frequency band may not reflect oscillatory activity.

232 Recommendations

233 Investigations of oscillations should start with a *detection* step, verifying the presence of
234 oscillations of interest. This verification step can be done in both the frequency and time domains.
235 In the time domain, visualizing the data allows for examining if there are clear rhythmic segments
236 in the data. In the frequency domain, oscillations manifest as peaks of power over and above the
237 aperiodic signal (Buzsáki et al., 2013). As an initial check, visually inspecting power spectra can
238 help to verify the presence of prominent oscillations. Including figures of power spectra in
239 manuscripts is recommended, as it provides supporting evidence to the reader that there is
240 oscillatory activity in the data under study.

241

242 Numerous quantitative methods also exist to detect oscillatory activity in neural field data,
243 such as automated methods that detect narrowband spectral peaks (Pascual-marqui et al., 1988).
244 This can be systematically done by parameterizing the power spectrum, in which a mathematical
245 model that quantifies periodic and aperiodic activity is applied to detect any putative oscillatory
246 peaks above the measured aperiodic component (Donoghue, Haller, et al., 2020) (see Fig. 1F).
247 Similarly, the 'extended better oscillation detection' (eBOSC) method (Kosciessa et al., 2020), an
248 extension of prior methods (Caplan et al., 2015; Whitten et al., 2011), uses a fit of the aperiodic
249 activity to threshold and detect frequency specific activity. It may also be useful to examine
250 rhythmic properties of the data, to search for putative oscillatory activity in situations in which a
251 spectral peak may be difficult to observe (Pesaran et al., 2018). One approach to do so is lagged
252 coherence (Fransen et al., 2015), which explicitly quantifies the rhythmicity in time series in
253 contrast to measuring solely spectral power, and can also be used to differentiate between
254 oscillatory signals and transients (see Fig. 1A). Time domain and burst burst detection methods,
255 further described in sections 4 and 5, may also be applicable.

256

257 Because oscillations can vary in their presence within and between participants, and
258 across different frequency bands (Donoghue, Haller, et al., 2020; Frauscher et al., 2018)

259   oscillation detection should be performed for each frequency band of interest, participant and

260   analyzed region. Group-level analyses may obscure variation in oscillatory presence in individual

261   participants. For example, if not all participants display a clear rhythm, effect size estimates of

262   oscillatory changes at the group level may be confounded by including the subset of participants

263   without any clear oscillatory activity. Alternately, a comparison of oscillatory power between

264   regions without doing oscillation detection may conflate a change in oscillatory power with a

265   difference in oscillatory presence. Analyses that include filtering or band-specific measures

266   without first examining if an oscillation is present can provide ambiguous results that may reflect

267   aperiodic activity, in which case it is a misinterpretation to describe physiological *oscillatory*

268   activity. Applying analyses to detect oscillatory presence can assure that measures reflect

269   oscillatory activity.

270

271   [APPROXIMATE LOCATION – FIGURE 1]

272

273 ## #2 Neural oscillations vary in their peak frequencies

274 *Why this matters*

275   Neural oscillations display significant variations in their peak frequencies, including
276 variation across age (Lindsley, 1939), within and between participants (Haegens et al., 2014),
277 and across cortical locations (Mahjoory et al., 2020). Alpha peak frequency, for example, is
278 considered a stable trait marker (Grandy et al., 2013), and is also associated with some clinical
279 disorders, displaying, for example, a slower frequency in attention-deficit hyperactivity disorder
280 (ADHD) (Lansbergen et al., 2011). The frequency of neural oscillations can also vary within
281 participants within a task (Benwell et al., 2019), including in task relevant ways (Wutz et al., 2018).
282

283   Due to frequency variation, even if the presence of oscillations is verified, the use of
284 canonically defined frequency ranges may still fail to accurately reflect the data, as this may
285 misestimate power of an oscillation if the spectral peak is not well captured in the canonical range.
286 For example, in Figure 2, a canonically defined alpha range of 8-12 Hz captures the peak of a 10
287 Hz oscillation (Fig. 2A), but fails to accurately capture a 8 Hz peak (Fig. 2B). Despite the signals
288 being simulated with the same amount of oscillatory power, estimated alpha power using a
289 canonical frequency range differs between the signals (Fig. 2C), due to an underestimate of the
290 power in the signal with an idiosyncratic peak frequency. This issue also impacts the result of
291 band-pass filtering, as a canonical filter range underestimates the amount of alpha power present,
292 as compared to an individualized band in which the filter range is made to reflect the oscillation
293 in the data (Fig. 2D). Using individualized frequency band ranges to control for frequency
294 differences accurately captures the alpha power in each signal (Fig. 2E). Overall, predefined
295 frequency band definitions may fail to address variation in peak frequencies, and lead to
296 misestimations.
297

298   Potential differences in peak frequency are important for analyses that compute an
299 estimate within a specific frequency range, such as calculating band power, or narrowband
300 filtering to a frequency range of interest. Applying a fixed frequency range may lead to information
301 loss when the individual peak frequency lies near the border or outside of the defined range; it
302 can also be non-specific if the range captures an adjacent oscillation or aperiodic activity. These
303 issues apply both to analyses of individual frequency bands, as well as to composite measures
304 such as ratios computed between the power of different frequency bands, since variation in the
305 peak frequency or bandwidth of peaks can impact measured results (Donoghue, Dominguez, et

306   al., 2020). For example, what had previously been reported as a difference in the theta / beta ratio

307   of participants with ADHD was found to be partially driven by a slowed alpha peak in the ADHD

308   group, changing the interpretation of the data (Lansbergen et al., 2011).

309   Recommendations

310   In order to address the variability of peak frequencies, any analyses that employ

311   narrowband frequency ranges should assess how well the chosen ranges match the data. Visual

312   inspection can help determine how well the defined frequency boundaries reflect actual peaks in

313   the power spectra. This should be done for all analyzed frequency bands at the level of individual

314   participants, because individual participants may have idiosyncratic peak frequencies that could

315   influence group level results if they are misestimated. For within-subject analyses, changes in

316   peak frequency over time or between tasks should also be considered in order to address whether

317   a measured change in power could reflect a change in peak frequency, in which frequencies may

318   'drift' outside defined ranges of interest. Including power spectra in manuscripts also enables

319   readers to observe that applied band ranges match the peaks observed in the data.

320   If chosen band ranges of interest do not appropriately reflect the data, then individualized

321   frequency bands may be applied (Klimesch, 1999). Methods for computing individualized

322   frequency bands often do so by measuring spectral peaks (Haegens et al., 2014; Pascual-marqui

323   et al., 1988). Automated approaches have also been developed, that include spectral smoothing

324   to improve performance (Corcoran et al., 2018). Such approaches don't always generalize to

325   multiple peaks or bands, though some approaches use 'anchor frequencies' (Klimesch, 1999),

326   defining, for example, theta as a range below the identified range of alpha. This approach has the

327   limitation of not considering the oscillation detection step. Peak detection for multiple putative

328   peaks, without predefining frequency ranges, can also be done with spectral parameterization

329   (Donoghue, Haller, et al., 2020), after which peaks can be grouped into observed bands of

330   interest.

331   Beyond spectral peak detection, methods for detecting oscillations can be used to detect

332   frequencies with peak rhythmicity, for example, by applying lagged coherence across frequencies

333   (Fransen et al., 2015). Some methods also allow for jointly learning multiple band definitions. For

334   example, the Oscillation ReConstruction Algorithm (ORCA) evaluates multiple band definitions in

335   terms of how well each definition is able to reconstruct the data (Watrous & Buchanan, 2020),

336   and the gedBounds method identifies frequency boundaries by clustering similarities across

337 frequencies (Cohen, 2021). These methods, which examine all analyzed frequencies together,

338 may help to obtain more consistent groups frequency ranges within and across participants.

339 Collectively, some form of evaluation needs to be done to verify frequency bands, in order to

340 ensure that applied measures accurately capture the intended oscillatory activity.

341

342   [APPROXIMATE LOCATION – FIGURE 2]

343

#3 Neural oscillations coexist with aperiodic activity

Why this matters

As previously introduced, neural field recordings contain aperiodic activity (B. J. He, 2014). This activity is not only ubiquitously present, but is also variable and dynamic within and between subjects (Freeman & Zhai, 2009; Podvalny et al., 2015). Between subject variability of aperiodic activity can relate to age (W. He et al., 2019; Voytek et al., 2015), and clinical diagnoses (Robertson et al., 2019), whereas within subjects, aperiodic activity varies with state, such as sleep (Lendner et al., 2020), relates to behavioural tasks (Podvalny et al., 2015) and can be influenced by exogenous stimuli and cognitive demands (Waschke et al., 2021). This dynamic aperiodic activity has different putative generators, physiological interpretations, and task related dynamics (Gao et al., 2017, 2020; K. J. Miller et al., 2009, 2014), as compared to oscillations, making it an interesting feature of interest in itself. Altogether, aperiodic neural activity is dynamic in many contexts in which neural oscillations are usually the focus of inquiry.

This dynamic quality of aperiodic activity is an important consideration for detecting neural oscillations, as previously discussed (see #1), as well as for interpreting measured changes in the data. With multiple dynamic components, analyses must adjudicate which aspects of the data are changing, and how, in order to allow for appropriate interpretations. Since aperiodic activity has power at all frequencies, changes or differences in aperiodic activity can induce patterns of differential activity across all frequencies. This can be seen by comparing white (χ = 0) and pink (χ = 1) noise $1/f^\chi$ signals, which have different amounts of power in a canonically defined alpha-band (Fig. 3A). Even with a validated spectral peak and frequency range, a difference in band-power between two conditions within a given frequency range may not be specific to oscillatory changes, as it may reflect a global change in aperiodic activity. For example, in Fig. 3B, a measured difference in alpha-band power between two conditions reflects a change in the aperiodic exponent, not changes relating to a spectral peak in the alpha-band.

Considering aperiodic activity is particularly important for analyses that investigate band-power across a series of frequency bands, since systematic patterns of measured changes across bands may not reflect any changes in oscillatory activity. For example, in Fig. 3C, the band-power of two conditions is compared across five different frequency bands. Despite this analysis suggesting a pattern of changes in band power across a series of canonically defined frequency

376   bands (Fig. 3D), the changes are actually driven by a change in aperiodic activity. Patterns of

377   correlated changes across frequency bands can therefore sometimes be more parsimoniously

378   explained by a change in aperiodic activity, rather than as multiple distinct oscillatory changes, as

379   has been shown to be the case in development (W. He et al., 2019).

380

381   Changes in global power, due to aperiodic changes, can also impact relative or normalized

382   measures of oscillatory activity. In the spectra in Fig 3D, there is a visible spectral peak in the

383   alpha-band. Even though there is no change in peak power, a relative power measure suggests

384   a change in alpha power, due to a change in the total power, that is driven by a change in aperiodic

385   activity (Fig. 3E). This issue also impacts other compound measures, such as ratios of band-

386   power, including the theta/beta-ratio, often investigated as a potential biomarker for ADHD

387   (Lansbergen et al., 2011; Robertson et al., 2019), as it has been shown that band ratio measures

388   often reflect a change of the aperiodic activity (Donoghue, Dominguez, et al., 2020), and that the

389   putative relationship between ADHD and theta/beta-ratio appears to be driven by aperiodic

390   activity (Robertson et al., 2019).

391   Recommendations

392   As both oscillatory and aperiodic components are dynamic, it is important for analyses to

393   validate which elements of the data are specifically changing, in order to appropriately interpret

394   results. This is relevant for any analysis investigating putative narrowband power, including

395   investigations that examine multiple oscillation bands. Aperiodic activity should be explicitly

396   measured to evaluate whether it explains the band-specific changes, including whether correlated

397   patterns of changes across frequency bands may be more parsimoniously explained as a change

398   in the broadband aperiodic activity. Approaches that assume oscillations exist upon a stationary

399   'background', such as relative power measures that divide by total power, or band ratio measures,

400   should be avoided, as they conflate changes in oscillatory and aperiodic components (Donoghue,

401   Dominguez, et al., 2020). For example, a change in a relative power metric that divides by total

402   power could arise from a change in band-specific power of interest, or be due to a change in

403   aperiodic component that changes the measured total power.

404

405   Explicitly measuring aperiodoc activity requires methods that explicitly conceptualize both

406   aperiodic and periodic activity, to avoid erroneously attributing aperiodic activity as oscillatory

407   changes. Methods that define and measure oscillatory activity relative to aperiodic activity,

408   including previously introduced methods such as spectral parameterization (Donoghue, Haller, et

Oscillation Methods

409   al., 2020) and eBOSC (Kosciessa et al., 2020), are designed to measure and control for aperiodic

410   activity, and so address this issue. There are also dedicated methods for measuring aperiodic

411   activity. For example, the irregular-resampling auto-spectral analysis (IRASA) method leverages

412   the scale-free nature of aperiodic activity by proposing a resampling procedure to isolate aperiodic

413   activity (Wen & Liu, 2016). IRASA can be used to separate and measure aperiodic neural activity,

414   after which analyses can evaluate each component to examine whether measures of interest

415   specifically reflect the intended component. Overall, controlling for aperiodic activity requires

416   employing an oscillation detection step and evaluating oscillatory power relative to the aperiodic

417   component in order to assess whether measured changes are capturing oscillatory or aperiodic

418   activity.

419

420   [APPROXIMATE LOCATION – FIGURE 3]

421

422 # #4 Neural oscillations are variable across time

423 Why this matters

424   Neural oscillations often display burst-like temporal dynamics (Lundqvist et al., 2016;
425 Sherman et al., 2016) and are rarely, if ever, completely consistent and continuous. These
426 temporal dynamics of neural oscillations are a potentially important feature; for example, the rate
427 of burst events has been found to be predictive of behavior across tasks and species (Shin et al.,
428 2017), including in investigations of working memory (Lundqvist et al., 2016) and motor activity
429 (Wessel, 2020). Some generative models of oscillations predict non-continuous events in a way
430 that is consistent with what is seen in empirical data (Sherman et al., 2016).

431

432   Despite this, many methods implicitly assume stationarity of the signal under study, when
433 analyzing, for example, average band power across time or trials. In such cases, variability of
434 oscillation presence or temporal dynamics can be misinterpreted as differences in power. For
435 example, in simulated signals with stochastic onset and offset of oscillatory activity, there can be
436 a different proportion of the data with oscillatory activity (Fig. 4A). Measured power in such cases
437 reports a different amount of band specific power, typically interpreted as reflecting a change in
438 the overall amplitude of the oscillation, however, measured differences can be due to temporal
439 variability (Fig. 4B). These kinds of averaging effects are also important in scenarios such as time-
440 frequency analyses that average across trials, which may create an illusion of sustained activity
441 in averaged data (Feingold et al., 2015; Jones, 2016). This can happen if individual trials have
442 burst-like temporal dynamics that occur at different times across different trials, which can
443 average together in a way as to suggest a sustained response in average data, despite such
444 continuity not occurring in any individual trial (Fig. 4C). The temporal variability of neural
445 oscillations motivates the importance of considering single trial dynamics (Kosciessa et al., 2020;
446 Stokes & Spaak, 2016).

447

448   Oscillatory bursts can vary in multiple ways that can lead to similar measured changes in
449 band power, which may be misinterpreted as reflecting changes in tonic band power. This
450 includes changes in burst duration (Fig. 4D), burst occurrence (Fig. 4E), or burst amplitude (4F),
451 each of which can vary within or between analyzed time periods (Quinn et al., 2019; Zich et al.,
452 2020). Understanding the different sources of variability has implications on how these signals
453 should be interpreted, as a change in the length, number or size of bursts each likely reflect

454   different circuit mechanisms and putative relationships to neural function. However, this can not
455   be appropriately evaluated unless methods acknowledge oscillations as potentially transient, with
456   potential variability in rate, timing, and duration as well as amplitude (van Ede et al., 2018).

457   Recommendations

458   Analyses of neural oscillations must therefore evaluate whether temporal variability, rather
459   than overall power, may be driving measured changes. In order to address temporal variability,
460   both the spectral and temporal domain have to be considered together (Zich et al., 2020). Time-
461   frequency analyses, such as spectrograms, can be used to examine spectral properties across
462   time in order to adjudicate between changes in the average power of oscillations and changes in
463   their temporal dynamics. In doing so, it is important to analyze single-trials (Stokes & Spaak,
464   2016), to avoid misinterpreting averaged power. If reporting spectrograms, single-trial examples
465   should be included in order to evaluate whether apparent sustained activity is truly sustained, or
466   arises as a result of averaging many short bursts.

467   Burst detection methods can also be applied to identify segments of the signal in which
468   oscillations are present, which can then be characterized in terms of the durations of the bursts,
469   the number of bursts, and/or the amplitude of the bursts. A common approach for burst detection
470   is to use an amplitude threshold, detecting segments of power in which frequency specific power
471   is greater than a chosen threshold level (Feingold et al., 2015). The previously described eBOSC
472   algorithm (Kosciessa et al., 2020) can be considered to be a threshold based burst detection, in
473   which the threshold is based on the aperiodic component, and can be used for burst detection.

474   Other algorithms for burst detection include matching pursuit, in which a dictionary of
475   atoms, which can include oscillatory bursts, is fit to the data, providing potentially more accurate
476   estimates of burst onset and duration (Chandran KS et al., 2018). Alternatively, methods such as
477   hidden markov modelling can be used, which seek to characterize state transitions, and can be
478   used to model transitions into and out of oscillatory states in a probabilistic way (Quinn et al.,
479   2019; Vidaurre et al., 2016). Time-domain measures that identify oscillations by characterizing
480   individual cycles, further described in #5, can also be used to detect and analyze the number and
481   duration of bursts, and their cycle-by-cycle properties (Cole & Voytek, 2019; Schaworonkow &
482   Nikulin, 2019). After detection, analyses of burst-like neural activity typically involve subsequent
483   analysis of the identified bursts, in order to evaluate whether they are changing in their duration,
484   occurrence, and/or amplitude.

485

486   [APPROXIMATE LOCATION – FIGURE 4]

487

#5 Neural oscillations are non-sinusoidal

489   Why this matters

490   The waveform shape of neural oscillations is often non-sinusoidal (Cole & Voytek, 2017;
491   Jones, 2016), as seen, for example, in the arc-shaped sensorimotor mu-rhythm, visual alpha,
492   which can be triangular, and the sawtooth-shaped hippocampal theta-rhythm. These waveform
493   properties of neural oscillations may reflect physiological properties, for example the
494   synchronization of neural activity (Schaworonkow & Nikulin, 2019), spiking patterns of underlying
495   neurons (Cole & Voytek, 2018), or behavioural correlates such as running speed (Ghosh et al.,
496   2020). Waveform shape can therefore be an important feature of interest, with potential to impose
497   constraints on generative circuit models of oscillations (Sherman et al., 2016) as well as time
498   constants of involved synaptic currents.

499   The variable waveform shape of oscillations also creates substantial methodological and
500   interpretation hurdles, due to the assumed sinusoidal basis underlying most methods. For
501   instance, estimating instantaneous phase typically involves narrowband filtering the signal before
502   applying a Hilbert transform. Applying a narrowband filter on data with variations in waveform
503   shape can be problematic, as the phases of sinusoidal outputs of narrowband filtering will not
504   correspond to phases of a non-sinusoidal signal (Fig. 5A). This occurs because in the spectral
505   domain, nonsinusoidal shapes are represented by power across multiple frequencies, and if the
506   signal content in the harmonic frequencies is removed, the resulting filtered signal will have shifted
507   peaks and troughs compared to the original non-sinusoidal signal (Fig. 5A). This is an important
508   consideration for any analyses that examine cycle properties, such as the location of signal peaks
509   and troughs, as putatively corresponding to specific physiological states. For analyses that rely
510   on exact temporal characteristics (e.g. investigating the effects of pre-stimulus phase on
511   behavioral measures), controlling for waveform shape may be beneficial.

512   In spectral analysis, non-sinusoidal waveforms are reflected in the power spectrum as
513   harmonics occurring at multiples of the dominant frequency, as illustrated in Fig. 5B. This can
514   result in interpreting these separate peaks as independent physiological rhythms. In the case of
515   an arc-shaped mu-rhythm, for example, the waveform shape of the oscillation will create peaks
516   in both the alpha- and beta-frequency ranges. This may be interpreted as separate alpha- and
517   beta-rhythms with an assumed phase- and amplitude-coupled relationship, when in reality only
518   one non-sinusoidal rhythm is present. Differentiating between those situations is complicated by

519   the fact that several types of rhythms can be found across the cortex (see section #6). Fig. 5C

520   shows how the degree of non-sinusoidality is reflected in the power of harmonic frequencies, with

521   higher power in the harmonic frequency range for increasing non-sinusoidality. This should be

522   considered when evaluating differences in spectral power between conditions, to control for

523   potential changes in waveform shape.

524   The spurious coupling that waveform shape can induce between frequencies (Kramer et

525   al., 2008) is especially important when considering measures such as phase-amplitude coupling

526   that are greatly influenced by waveform shape (Cole et al., 2017; Lozano-Soldevilla et al., 2016).

527   Waveform shape can result in systematic changes in the amplitude at harmonic frequencies, as

528   seen in Fig. 5D, which can depend on the phase of the base oscillation, as quantified in Fig. 5E.

529   This results in significant measures of cross-frequency phase-amplitude coupling. Numerically,

530   these values are not objectionable, as they reflect a relationship between frequencies in the

531   spectral domain. However, there is possible fallacy in the interpretation, if this relationship is taken

532   to reflect significant coupling between *independent* rhythms, when in fact no such interaction

533   between multiple rhythms need exist. Because of these methodological limitations, careful work

534   needs to be done to adjudicate between phase amplitude coupling measures that reflect

535   waveform shape versus those that truly reflect nested oscillations (Giehl et al., 2021; Vaz et al.,

536   2017).

537   Recommendations

538   In order to evaluate and control for waveform shape, explicit measurement of waveform

539   and cycle properties should be done. Time domain measures of individual cycles can be used to

540   characterize waveform shape by, for example, calculating measures such as the rise/decay

541   symmetry or peak sharpness (Cole & Voytek, 2019; Schaworonkow & Nikulin, 2019). Other

542   methods aim at learning and grouping waveforms into observed categories, for example through

543   attempting to learn recurring patterns in the data by sliding-window matching (Gips et al., 2017)

544   or by attempting to learn a dictionary of observed shapes in the data and finding occurrences of

545   particular waveforms in the data based on templates (Barthélemy et al., 2013; Brockmeier &

546   Principe, 2016; Jas & Dupré, 2017).

547   In the frequency domain, specific waveforms can create stereotypical patterns in power

548   spectra and time-frequency representations, which can complicate the detection of oscillations

549   (see #1). If spectral peaks are present at exact multiples of slower frequencies, quantifying

550   waveform shape may help to distinguish between an independent oscillation at that particular

551 frequency or harmonic spectral peaks induced by waveform shape. Since different waveform
552 shapes may exhibit similar time-frequency representations (Jones, 2016), time-domain analyses
553 may be required to evaluate if and how waveform shape is contributing to spectral
554 representations.

555 For cross-frequency coupling analysis, the frequency extent of local coupling within a
556 region (e.g., for phase amplitude coupling, the range of higher frequencies that are coupled to the
557 low frequency phase) can suggest whether it is likely to be genuine oscillatory coupling or a shape
558 effect (Cole et al., 2017; Vaz et al., 2017), with narrow ranges at exactly multiples of the base
559 frequencies indicative of possible coupling caused by waveform shape. Applying and comparing
560 multiple measures of cross-frequency coupling can dissociate harmonic and non-harmonic
561 phase-amplitude coupling (Giehl et al., 2021). More generally, frequency domain methods such
562 as bicoherence, a measure of non-linear interactions between frequencies, can also be used to
563 investigate waveform shape in the frequency domain (Bartz et al., 2019).

564

565 [APPROXIMATE LOCATION – FIGURE 5]

566

567 # #6 Multiple oscillations coexist across the brain

568 Why this matters

569   Non-invasive recordings of neural oscillations reflect aggregate activity across relatively
570 large cortical areas. Through volume conduction, a term used to describe the propagation of
571 electrical fields from their original source across tissues to recording sensors, recording
572 electrodes can reflect activity from multiple local sources, as well contributions from more distant
573 sources that overlap both spatially as well as temporally (Buzsáki et al., 2012; Nunez &
574 Srinivasan, 2006). For instance, in the context of MEG/EEG, there are several alpha-rhythm
575 sources, with locations in somatosensory, occipital, parietal and temporal cortex (Hindriks et al.,
576 2017), which can be co-active at the same time. In many studies, recordings are analyzed in
577 sensor space, by directly analyzing activity from recording electrodes. In such cases, the
578 aggregate signal may appear markedly different from the underlying sources of interest due to
579 the spatial and temporal overlap of multiple distinct sources. Measures applied to these combined
580 signals may therefore not accurately reflect the underlying sources, with distortions in measures
581 of temporal dynamics or waveform shape (Schaworonkow & Nikulin, 2019).

582

583   We demonstrate how spectral and time domain measures can be affected in an example
584 in which sensor space activity from a single electrode is composed of activity from two underlying
585 sources in the parietal and visual cortices (Fig. 6A). In the spectral domain, this configuration can
586 result in two peaks in the alpha-frequency range (Fig. 6B), when the two sources have slightly
587 different peak frequencies. This has been observed in empirical data as 'double alpha' or 'split
588 alpha' peaks (Chiang et al., 2008). Analyses in sensor space may lead to the interpretation that
589 a specific circuit generates signals with two simultaneously present peak frequencies, which in
590 turn will influence theories of generating mechanisms. Spatial summation of multiple underlying
591 rhythms of similar peak frequencies can also mask temporal features of interest of the underlying
592 rhythms, as seen in Fig. 6C, due to constructive and destructive interference effects
593 (Schaworonkow & Nikulin, 2019). Phase differences between sources of similar frequencies can
594 attenuate the oscillation in sensor space, due to interference, even though oscillatory power has
595 not changed in the underlying sources. This may lead to erroneous interpretations regarding
596 changing oscillatory power of the sources, when it may be that only their relative temporal
597 relationship has changed.

598

599   Inter-regional connectivity measures are also impacted by the simultaneous presence of
600   multiple sources. Computing connectivity measures using sensor space signals can lead to
601   spurious findings, because volume conduction influences these measures (Haufe et al., 2013; J.
602   M. Palva et al., 2018; S. Palva & Palva, 2012; Schoffelen & Gross, 2009). Because individual
603   sources propagate to multiple sensors, regularities in amplitude and phase will be present across
604   multiple sensors. This can yield highly significant statistical relationships between electrodes,
605   reflecting signal content that is present due to a common source rather than genuine interregional
606   coupling, which may lead to erroneous interpretation of connectivity between oscillatory sources.

607   Recommendations

608   Due to overlapping sources, analyzing sensor level time series or power spectra can be
609   misleading regarding which aspects of the oscillation are present and/or are changing. Whenever
610   possible, sensor space analysis should be complemented by source-level analysis. Source
611   separation methods can be applied to attempt to separate different narrowband periodic
612   components in the signal, which can help to reveal features that are not visible in sensor space
613   data, as well as helping to localize sources. There are many possible approaches for source
614   separation. Because inferring the activity of many more sources than channels is not possible,
615   constraints are needed to arrive at a specific decomposition. For example, anatomical information
616   can be used to constrain the inverse solution based on individual or template structural MRI, in
617   combination with methods such as beamformer or minimum norm estimation techniques (Hauk
618   et al., 2019).

619

620   For estimating source time series in order to potentially separate oscillatory sources, there
621   is a class of approaches that explicitly use the statistical structure across channels. In this
622   approach, channel activity is assumed to be a linear mixture of multiple underlying sources,
623   defined by a leadfield matrix, which describes how individual sources map onto sensors (Parra et
624   al., 2005). By assuming specific statistical properties of the source time series as well as mixing
625   properties, demixing can be attempted. Methods in this realm include joint decorrelation (de
626   Cheveigné & Parra, 2014) or independent component analysis (Hyvärinen & Oja, 2000). In the
627   context of investigating neural oscillations, there are variants that specifically maximize SNR of
628   narrowband oscillatory components, while minimizing SNR in flanking bands or in comparison to
629   broadband activity. For enhancing oscillatory SNR, spatial-spectral decomposition (Nikulin et al.,
630   2011) or generalized eigendecomposition (Cohen, 2017b) can be used. The Common Spatial
631   Patterns algorithm (Koles, 1991) and it's variants (Lotte & Cuntai Guan, 2011) can be used for

632 maximizing differences in narrowband activity between task conditions. For investigating
633 relationships between narrowband activity and a continuous variable, Source Power Correlation
634 analysis (Dähne et al., 2014) may be of interest. Spatial filtering methods can also be used as a
635 preprocessing step for dimensionality reduction (Haufe, Dähne, et al., 2014), easing statistical
636 comparisons and computational needs.

637 Components that result from source separation need validation, since different methods
638 or parameter settings can yield highly different results, and solutions are not guaranteed to reflect
639 physiologically meaningful activity. As such, source separation can be non-trivial and has its own
640 set of methodological considerations as well as reporting guidelines (Cohen & Gulbinaite, 2014;
641 Haufe, Meinecke, et al., 2014; Mahjoory et al., 2017). These guidelines can be used to evaluate
642 robustness of the solution, such as with goodness of fit and/or localization error metrics, and to
643 adequately convey reconstruction quality and method details to the reader.

644

645 [APPROXIMATE LOCATION – FIGURE 6]

646

647 ## #7 Measures of neural oscillations require sufficient signal-to-noise ratio

648 Why this matters

649   Neural oscillations are embedded in complex recordings containing multiple rhythmic
650 signals, aperiodic activity, and transient events. Analyzing oscillatory signals of interest requires
651 defining features of interest (signal), and extracting this signal from the rest of the data (noise).
652 As with all measures, methods for analyzing oscillations require an adequate signal to noise ratio
653 (SNR). Indeed, ubiquitous processing steps such as filtering are used largely in order to increase
654 the SNR (Widmann et al., 2015). Many of the considerations thus far (detecting oscillations,
655 adjusting frequency ranges, controlling for aperiodic activity, burst detection, and source
656 separation) can all be conceptualized as aiming to increase SNR.

657   The SNR of oscillatory activity relates to the ratio of oscillatory power to noise, typically
658 the aperiodic background. Oscillatory power is a dynamic property, which can be seen by the
659 variable height of oscillatory peaks over and above the aperiodic component (Fig. 7A). Many
660 experimental paradigms will change oscillatory power, as presentation of stimuli may result in
661 event-related attenuation of oscillations (Pfurtscheller & Lopes da Silva, 1999). This change in
662 oscillatory power changes SNR, which in turn may influence accuracy and stability of other
663 oscillatory measures such as instantaneous phase and frequency. When SNR is high, estimations
664 of phase and frequency can be reliably estimated (Fig. 7B). However, when SNR is low,
665 estimation can be very noisy (Sameni & Seraj, 2017) as can be seen in Fig. 7C, leading to
666 artifactual large variations, often referred to as phase slips.

667   Changes in oscillatory power which change SNR and corrupt phase estimations can lead
668 to inaccurate estimates of derived measures, such as the phase-locking value
669 (Muthukumaraswamy & Singh, 2011). Low SNR makes it difficult to reliably extract oscillations of
670 interest (Fig. 7D), leading to variable phase estimates (Fig. 7E). When computing coupling
671 measures on such estimates, differences in SNR, absent any true changes in phase alignment,
672 can erode the detection of phase-locking between two signals (Fig. 7F). Unstable estimation of
673 oscillatory measures can also propagate to multivariate analysis, such as cross-frequency
674 coupling, whereby oscillatory power changes that influence SNR can lead to a change in
675 measured cross-frequency coupling (Aru et al., 2015). Time domain analyses, such as those
676 designed for analyzing waveform shape, are also strongly dependent on their being adequate
677 SNR to meaningfully measure the properties of interest.

678   In cases of low SNR, unreliable estimates could, for example, lead to false-negatives due
679   to noisy estimations that are not able to adequately capture measures of interest. Conversely,
680   certain analyses may return false positive results, if the measured variability of the signal is mis-
681   intepreted as a feature of interest, and/or leads to an artifactual measured change between
682   conditions due to variable SNR. This may be an issue when comparing between groups who are
683   known to have differences in relative power of oscillations, and/or when comparing within
684   participants across conditions that may have different SNR.

685   Recommendations

686   Considering the SNR required for stable estimation of measures of oscillations starts by
687   choosing appropriate experimental designs. When designing the protocol and tasks,
688   experimenters should consider what is known about the reliability and effect size of effects of
689   interest, and consider doing a power analysis to design well powered studies. This includes
690   considering recording modalities, as different modalities have different sensitivities to different
691   source locations (Piastra et al., 2020), as well as the different temporal, spatial, and frequency
692   resolutions they offer. When recording the data, best practices should be employed to minimize
693   non-neuronal noise, and use appropriate preprocessing in order to increase the quality of the data
694   with the respect to desired analyses (Keil et al., 2014; Pernet et al., 2020).

695   Once data are recorded, or if considering existing datasets for potential re-analysis, signal-
696   to-noise ratio has to be considered to validate if the dataset is appropriate for the desired
697   analyses. This requires explicitly measuring SNR to verify that applied measures are robust in the
698   SNR regime of the data. If the SNR is too low to provide accurate measurements, the analyses
699   may be non-viable, as any measurements will be uninterpretable. If the analysis can be run, then
700   SNR should still be continuously verified, to evaluate whether potential changes of SNR across
701   time or between conditions may explain measured changes in results.

702   General approaches for optimizing SNR include good filter design (de Cheveigné &
703   Nelken, 2019; Widmann et al., 2015), and using information about spectral estimators and signals
704   of interest to select the most appropriate methods to improve the accuracy and stability of
705   estimates (Chavez et al., 2006; Lepage et al., 2013). There are also specific methods for more
706   robust estimations of phase in low power situations, including Monte Carlo estimation (Sameni &
707   Seraj, 2017) and smoothing via Kalman filtering (Mortezapouraghdam et al., 2018). Many of the
708   previously described methods such as detecting oscillatory peaks, using individualized frequency

709 ranges, and using burst detection can all improve SNR. Source separation techniques, including

710 those that explicitly optimize SNR (Cheveigné & Arzounian, 2015; Nikulin et al., 2011) can be

711 used to extract oscillatory components with higher SNR.

712   [APPROXIMATE LOCATION – FIGURE 7]

713

Discussion

714

715   How, and to what extent, neural oscillations are mechanistically involved in cognition
716   remains undetermined. This lack of clarity likely arises in part from imprecisions in our
717   methodological approaches for analyzing oscillations that, in turn, give rise to inconsistent results.
718   Here, we highlight specific methodological considerations for analyzing and interpreting neural
719   oscillations, providing explicit recommendations regarding each point. These considerations
720   acknowledge the heterogeneity of neural oscillations and embrace this complexity as an
721   opportunity to consider ideas and interpretations that may help us to further understand our data.
722   Oscillations vary in their presence and frequency, co-exist with dynamic aperiodic activity, have
723   idiosyncratic temporal and waveform shape properties, overlap with one another, and require
724   sufficient SNR to appropriately analyze. These topics also demonstrate that there is an increasing
725   set of features that can be defined for neural oscillations, with an increasing toolkit of estimation
726   methods. Hopefully, these recommendations can serve as guidelines for potentially reducing
727   misinterpretations and conflicting results, and can increase clarity in our understanding of neural
728   oscillations.

729

730   Though we present the considerations as seven distinct points, it is important to note that
731   they do not manifest in isolation from one another and can interact. For example, variable
732   aperiodic activity (#3) can complicate spectral peak (#1) and/or burst (#4) detection, as it
733   complicates approaches that use a threshold criterion to define bursts or spectral peaks;
734   oscillations may be difficult to detect (#1) and/or individualize frequencies for (#2) if they are
735   temporally rare (#4), due to low SNR (#7); waveform shape (#5) may systematically vary in
736   relation to underlying sources (#6) (Schaworonkow & Nikulin, 2019); and detected peaks (#1)
737   may be volume conducted from remote sources (#6), resulting, for example, in 'double alpha'
738   peaks due to the overlap of occipital and sensorimotor rhythms in the alpha-band (Chiang et al.,
739   2008). Multiple oscillatory features, such as power, waveform shape, burst rate, etc., can covary.
740   These potential multicollinearities need to be explicitly considered and tested by robust analyses
741   that control for multiple potentially confounding features, for example addressing overlapping
742   periodic and aperiodic activity (Donoghue, Haller, et al., 2020; Kosciessa et al., 2020), waveform
743   shape, which may result in spurious power- and/or phase-coupling (Cole & Voytek, 2019;
744   Schaworonkow & Nikulin, 2019), and examining trial-by-trial dynamics that may be masked or
745   conflated in average measures (Jones, 2016; Stokes & Spaak, 2016; Zich et al., 2020).

746

Oscillation Methods

747   This investigation used a simulation approach that attempts to mimic the properties seen
748 in empirical data, including dynamic aperiodic activity, and oscillatory components that can vary
749 across multiple features (Cole et al., 2019). Because ground-truth properties of physiological data
750 are not known in a way that can be used to evaluate the accuracy of applied measures, simulated
751 data are an important tool for diagnosing available methods. In using simulated data, we must
752 endeavor to reflect on our empirical data—simulating heterogeneous oscillatory features
753 embedded within dynamic aperiodic activity—in order to be representative of empirical data and
754 realistic use cases. As well as the tool used here, there are other approaches for simulating data,
755 including for specific modalities such as EEG (Krol et al., 2018) or MEG (Aine et al., 2012), or that
756 emulate neural circuits (Neymotin, Daniels, et al., 2020), or whole brain recordings (Sanz Leon et
757 al., 2013). Simulation analyses should be employed when developing new analysis approaches,
758 as novel methods require validation, and comparison to existing methods, such that best practice
759 guidelines can be continuously developed and updated. All time-frequency methods include
760 settings that should also be validated and explored. Sensitivity analyses, in which one repeats
761 the analyses across mild perturbations of method settings to evaluate the robustness of the
762 measured results, should be used to ensure that results are not overly dependent on specific
763 parameter regimes.

764

765   Estimates of oscillatory features of interest are typically further analyzed and compared
766 using statistical methods. Notably, many neuroscientific parameters exhibit skewed distributions
767 (Buzsáki & Mizuseki, 2014), including oscillatory power (Kiebel et al., 2005). Therefore,
768 distributional properties of data should be carefully considered such that appropriate statistical
769 tests can be chosen (Maris, 2012; Maris & Oostenveld, 2007). This is especially important when
770 considering that power-law distributed variables can result in spurious correlations when using
771 methods that assume normality (Schaworonkow et al., 2015). Statistical analyses, in particular in
772 the context of new methods and measures, should also evaluate consistency across participants
773 (Grice et al., 2020), reliability within participants, and effect size measures, which can be
774 computed using estimation statistics (Calin-Jageman & Cumming, 2019). Considering effect sizes
775 can also aid in designing studies that are sufficiently powered (Button et al., 2013). Adopting the
776 best practices proposed here may also help to increase statistical power, insofar as they help to
777 better and more specifically characterize features of interest, improving SNR.

778

779   In our examples, we focused primarily on univariate measures, such as estimating
780 oscillatory power or phase. Issues that affect these estimates also propagate to derived

781   measures, such as correlations between amplitude or phase, as is done in functional connectivity
782   (Haufe et al., 2013) and cross-frequency coupling analyses (Aru et al., 2015). If phase estimates
783   are unreliable due to low oscillatory SNR (Sameni & Seraj, 2017), or if amplitude estimates are
784   biased by changes in aperiodic activity (Donoghue, Haller, et al., 2020), or if burst properties vary
785   between analyzed signals (Jones, 2016), then derived measures may fail to reflect the intended
786   oscillatory properties. Methodological limitations are likely to propagate and compound in
787   multivariate or mass univariate analyses, and must therefore be considered for any analyses
788   including, or built on top, of the univariate methods demonstrated here.

789

790   Though beyond the scope of this article, investigations of neural oscillations also require
791   employing best-practices for designing, collecting, and preprocessing data in order to ensure
792   sound research design, high quality data, and methodological validity. These considerations are
793   covered in available textbooks (Cohen, 2014; Hari & Puce, 2017), as well as individual reports
794   that discuss topics such as including best practices for reporting and conducting MEG/EEG
795   research (Gross et al., 2013; Keil et al., 2014; Pernet et al., 2020), pre-processing (de Cheveigné
796   & Arzounian, 2018), artifact rejection and data cleaning (Jas et al., 2017; Urigüen & Garcia-
797   Zapirain, 2015), and guides to using common software tools such as MNE (Gramfort, 2013; Jas
798   et al., 2018) and FieldTrip (Oostenveld et al., 2011; Popov et al., 2018). Other work also features
799   dedicated discussion for specific methods such as filtering (de Cheveigné & Nelken, 2019;
800   Widmann et al., 2015), phase estimations (Chavez et al., 2006; Lepage et al., 2013), functional
801   connectivity (O'Neill et al., 2018), and cross-frequency coupling analyses (Aru et al., 2015).

802

803   Broader strategies are also required for addressing reproducibility in the field of neural
804   oscillations, including replication studies, providing clear descriptions of methods and results, and
805   publishing null results (Cohen, 2017a). Open-science practices, including making data and
806   analysis code available, can help foster reproducibility and develop transparency (Gleeson et al.,
807   2017; Kathawalla et al., 2020; Voytek, 2016). Due to their computational nature, investigations of
808   neural oscillations also benefit from good code practice (Wilson et al., 2017). Standardized
809   procedures for organizing datasets also increase shareability, organization, and can assist in
810   standardized pipelines, making it easier to apply novel methods (Holdgraf et al., 2019; Niso et al.,
811   2018; Pernet et al., 2019). Adopting open science practices provides opportunities for using open
812   tools and datasets that can foster transparency and efficiently allow for revisiting the evidence for
813   how neural oscillations relate to cognition and disease.

814

815   Importantly, these considerations also reflect opportunities for developing new theory and

816   understanding of neural field data, which is still in many ways a mystery (Cohen, 2017c). Aperiodic

817   activity is itself a physiologically informative feature (Gao et al., 2017, 2020), reflecting processes

818   distinct from neural oscillations (Chaoul & Siegel, 2020). New methods provide new opportunities,

819   for example, the ability to jointly analyze multiple components of the data, such as how oscillations

820   and aperiodic activity jointly contribute to cognitive processing (Cross et al., 2020). New features

821   of interest offer the potential for better understanding underlying physiology and putative

822   computational roles of neural oscillations. For example, modelling that explicitly considers

823   waveform shape and/or burst properties has contributed to physiological models of neocortical

824   beta generation (Sherman et al., 2016), and models proposing mechanisms of beta and gamma

825   activity in working memory (E. K. Miller et al., 2018).

826

827   Our emerging understanding of the data under study and how to measure it provides new

828   vistas of opportunity for continuing to understand neural field data, and how it relates to cognition

829   and disease. These methods and topics reflect the current status of methodological

830   considerations in oscillations work. As our understanding of the many complexities of neural data

831   continues to evolve, future investigations of neural oscillations must continue a consistent process

832   of interrogating the assumptions of our methods and how they relate to current knowledge of the

833   data to validate measures of the data, and develop evolving best practices.

834

835   Conclusion

836   Productively investigating neural oscillations requires dedicated and carefully applied
837   methods that reflect our current understanding of the data. As methodological validity is a
838   prerequisite for appropriate interpretation, analysis methods must reflect that neural field data
839   consists of a complex combination of multiple oscillatory components, variable aperiodic activity,
840   and transient events, within which oscillations vary across multiple dimensions. Here, we have
841   proposed a checklist of methodological considerations for neural oscillations, with
842   recommendations to 1) validate that oscillations are present; 2) verify that used frequency ranges
843   are appropriate; 3) control for potential confounds due to aperiodic activity; consider the 4)
844   temporal variation and 5) waveform shape of neural oscillations; 6) apply source separation, as
845   needed, to separate multiple oscillatory processes; and 7) evaluate that the SNR is adequate for
846   the analyses at hand. These considerations, and new methods that have been developed to
847   address them, reflect our emerging understanding of neural field data and offer new possibilities
848   for investigating, and ultimately, understanding, neural oscillations.

849

Materials and Methods

850

851   We employed a simulation-based approach to create the demonstrations in this

852 manuscript. Simulated time series were created with the NeuroDSP toolbox (Cole et al., 2019),

853 version 2.2.0. In most cases, the time series were created as a combination of oscillatory and

854 aperiodic activity, sampled at 1000 Hz. Oscillatory activity was simulated as sine waves unless

855 otherwise noted. Each oscillation was simulated at a specific frequency, typically in the alpha

856 band, unless otherwise specified. Aperiodic activity was simulated by spectrally rotating white

857 noise to the desired 1/f exponent (Timmer & Konig, 1995). Aperiodic and oscillatory signal

858 components were weighted according to a specified variance and combined together in an

859 additive manner. Across all analyses, power spectra were estimated using Welch's method

860 (Welch, 1967), using Hanning windowed 1 second segments with 12.5% overlap. Filtering was

861 done with finite impulse response bandpass filters, with linear phase and filter lengths set to a

862 default of 3 cycles of the highpass frequency, and enforced to be odd (Type I). Canonical band

863 ranges were defined as delta (2-4 Hz), theta (4-8 Hz), alpha (8-13 Hz), and beta (13-30 Hz),

864 unless otherwise specified. Analysis methods were also used as available in the NeuroDSP

865 toolbox,   or   with   custom   code   included   in   the   project   repository

866 (https://github.com/voytekresearch/oscillationmethods).

867

868   Several of the figure demonstrations used additional processing. For the peak detection

869 in Figure 1, the spectral peak was detected and quantified using spectral parameterization, which

870 models the power spectrum as a combination of aperiodic and oscillatory components, and can

871 be used to detects peaks of putative oscillatory power over and above the measured aperiodic

872 component (Donoghue, Haller, et al., 2020). For the individual frequency example in Figure 2,

873 canonical alpha was defined as +/- 2 Hz around 10 Hz, and individualized alpha bands were

874 defined as +/- 2 Hz around the individuals peak frequency. For the demonstrations of varying

875 aperiodic activity in Figure 3, generated time series were spectrally rotated, in the same manner

876 as done to simulate the aperiodic activity (Timmer & Konig, 1995). Relative power was computed

877 as the sum of power in a frequency band of interest, divided by the sum of power across all

878 frequencies in the frequency range of 2-50 Hz.

879

880   For the temporal variation demonstrations in Figure 4, bursty oscillations were simulated

881 by specifying time segments that should include an oscillation, optionally controlling the duration,

882 occurrence, and amplitude of the bursts. Burst specific power was calculated by sub-selecting

883   segments of the data with an oscillation present. For the examinations of waveform shape in
884   Figure 5, oscillations were simulated as asymmetric sine waves, and the bycycle toolbox (version
885   1.0.0) was used to quantify waveform shape in the time domain (Cole & Voytek, 2019). For this,
886   signals were band-pass filtered around the frequency of interest (here: 10 Hz) to extract the time
887   points zero-crossings of the signal. The time points were used to segment the broadband data
888   into cycles, determining several cycle parameters. For this example, we used simulated time
889   series with varying rise-decay symmetry, which is the ratio of time in the rising and decaying
890   segments of the oscillation, which creates asymmetric oscillations.

891

892   For the spatial mixing demonstration in Figure 6, the New York Head (ICBM-NY) was used
893   (Huang et al., 2016) as a head model. Two sources are placed in the posterior cortex, and the
894   corresponding sensor signals are calculated using the leadfield. Oscillations were simulated as
895   asymmetric waves, created as the sum of two sines waves with a fixed phase lag. Topographies
896   were visualized using MNE-python (Gramfort, 2013). In Figure 7, instantaneous measures were
897   computed by applying the Hilbert transform to signals bandpass filtered into the alpha range (8-
898   12 Hz), taking the angle as the phase estimate, and using the derivative of the instantaneous
899   phase as a measure of instantaneous frequency. Phase synchrony was measured using the
900   phase locking value (Lachaux et al., 1999).

901

902

34

References

904 Aine, C. J., Sanfratello, L., Ranken, D., Best, E., MacArthur, J. A., Wallace, T., Gilliam, K., Donahue, C.
905   H., Montaño, R., Bryant, J. E., Scott, A., & Stephen, J. M. (2012). MEG-SIM: A Web Portal for Testing
906   MEG Analysis Methods using Realistic Simulated and Empirical Data. *Neuroinformatics*, *10*(2), 141–
907   158. https://doi.org/10.1007/s12021-011-9132-z
908 Aru, J., Aru, J., Priesemann, V., Wibral, M., Lana, L., Pipa, G., Singer, W., & Vicente, R. (2015).
909   Untangling cross-frequency coupling in neuroscience. *Current Opinion in Neurobiology*, *31*, 51–61.
910   https://doi.org/10.1016/j.conb.2014.08.002
911 Babiloni, C., Barry, R. J., Başar, E., Blinowska, K. J., Cichocki, A., Drinkenburg, W. H. I. M., Klimesch, W.,
912   Knight, R. T., Lopes da Silva, F., Nunez, P., Oostenveld, R., Jeong, J., Pascual-Marqui, R., Valdes-
913   Sosa, P., & Hallett, M. (2020). International Federation of Clinical Neurophysiology (IFCN) – EEG
914   research workgroup: Recommendations on frequency and topographic analysis of resting state EEG
915   rhythms. Part 1: Applications in clinical research studies. *Clinical Neurophysiology*, *131*(1), 285–307.
916   https://doi.org/10.1016/j.clinph.2019.06.234
917 Barthélemy, Q., Gouy-Pailler, C., Isaac, Y., Souloumiac, A., Larue, A., & Mars, J. I. (2013). Multivariate
918   temporal dictionary learning for EEG. *Journal of Neuroscience Methods*, *215*(1), 19–28.
919   https://doi.org/10.1016/j.jneumeth.2013.02.001
920 Bartz, S., Avarvand, F. S., Leicht, G., & Nolte, G. (2019). Analyzing the waveshape of brain oscillations
921   with bicoherence. *NeuroImage*, *188*, 145–160. https://doi.org/10.1016/j.neuroimage.2018.11.045
922 Başar, E. (2013). Brain oscillations in neuropsychiatric disease. *Dialogues in Clinical Neuroscience*,
923   *15*(3), 291–300. https://doi.org/10.31887/DCNS.2013.15.3/ebasar
924 Başar, E., Başar-Eroglu, C., Karakaş, S., & Schürmann, M. (2001). Gamma, alpha, delta, and theta
925   oscillations govern cognitive processes. *International Journal of Psychophysiology*, *39*(2), 241–248.
926   https://doi.org/10.1016/S0167-8760(00)00145-8
927 Benwell, C. S. Y., London, R. E., Tagliabue, C. F., Veniero, D., Gross, J., Keitel, C., & Thut, G. (2019).
928   Frequency and power of human alpha oscillations drift systematically with time-on-task. *NeuroImage*,
929   *192*, 101–114. https://doi.org/10.1016/j.neuroimage.2019.02.067
930 Brazier, M. A. B. (1958). The Development of Concepts Relating to the Electrical Activity of the Brain. *The
931   Journal of Nervous and Mental Disease*, *126*(4), 303–321.
932 Brockmeier, A. J., & Principe, J. C. (2016). Learning Recurrent Waveforms Within EEGs. *IEEE
933   Transactions on Biomedical Engineering*, *63*(1), 43–54. https://doi.org/10.1109/TBME.2015.2499241
934 Bruns, A. (2004). Fourier-, Hilbert- and wavelet-based signal analysis: Are they really different
935   approaches? *Journal of Neuroscience Methods*, *137*(2), 321–332.
936   https://doi.org/10.1016/j.jneumeth.2004.03.002
937 Bullock, T. H., Mcclune, M. C., & Enright, J. T. (2003). Are the electroencephalograms mainly rhythmic?
938   Assessment of periodicity in wide-band time series. *Neuroscience*, *121*(1), 233–252.
939   https://doi.org/10.1016/S0306-4522(03)00208-2
940 Button, K. S., Ioannidis, J. P. A., Mokrysz, C., Nosek, B. A., Flint, J., Robinson, E. S. J., & Munafò, M. R.
941   (2013). Power failure: Why small sample size undermines the reliability of neuroscience. *Nature
942   Reviews Neuroscience*, *14*(5), 365–376. https://doi.org/10.1038/nrn3475
943 Buzsáki, G., Anastassiou, C. A., & Koch, C. (2012). The origin of extracellular fields and currents—EEG,
944   ECoG, LFP and spikes. *Nature Reviews Neuroscience*, *13*(6), 407–420.
945   https://doi.org/10.1038/nrn3241
946 Buzsáki, G., & Draguhn, A. (2004). Neural oscillations in cortical networks. *Science*, *304*(5679), 1926–
947   1929. https://doi.org/10.1126/science.1099745
948 Buzsáki, G., Logothetis, N., & Singer, W. (2013). Scaling Brain Size, Keeping Timing: Evolutionary
949   Preservation of Brain Rhythms. *Neuron*, *80*(3), 751–764. https://doi.org/10.1016/j.neuron.2013.10.002
950 Buzsáki, G., & Mizuseki, K. (2014). The log-dynamic brain: How skewed distributions affect network
951   operations. *Nature Reviews Neuroscience*, *15*(4), 264–278. https://doi.org/10.1038/nrn3687
952 Buzsáki, G., & Watson, B. O. (2012). Brain Rhythms and Neural Syntax: Implications for Efficient Coding
953   of Cognitive Content and Neuropsychiatric Disease. *Dialogues in Clinical Neuroscience*, *14*(4), 345–
954   367. https://doi.org/10.31887/DCNS.2012.14.4/gbuzsaki
955 Calin-Jageman, R. J., & Cumming, G. (2019). Estimation for Better Inference in Neuroscience. *Eneuro*,
956   *6*(4), ENEURO.0205-19.2019. https://doi.org/10.1523/ENEURO.0205-19.2019
957 Caplan, J. B., Bottomley, M., Kang, P., & Dixon, R. A. (2015). Distinguishing rhythmic from non-rhythmic

958   brain activity during rest in healthy neurocognitive aging. *NeuroImage*, *112*, 341–352.
959   https://doi.org/10.1016/j.neuroimage.2015.03.001
960   Chandran KS, S., Seelamantula, C. S., & Ray, S. (2018). Duration analysis using matching pursuit
961   algorithm reveals longer bouts of gamma rhythm. *Journal of Neurophysiology*, *119*(3), 808–821.
962   https://doi.org/10.1152/jn.00154.2017
963   Chaoul, A. I., & Siegel, M. (2020). *Distinct cortical correlation structures of fractal and oscillatory neuronal*
964   *activity* (p. 37) [Preprint]. bioRxiv. https://doi.org/10.1101/2020.12.10.415315
965   Chavez, M., Besserve, M., Adam, C., & Martinerie, J. (2006). Towards a proper estimation of phase
966   synchronization from time series. *Journal of Neuroscience Methods*, *154*(1–2), 149–160.
967   https://doi.org/10.1016/j.jneumeth.2005.12.009
968   Cheveigné, A. de, & Arzounian, D. (2015). Scanning for oscillations. *Journal of Neural Engineering*, *12*(6),
969   066020. https://doi.org/10.1088/1741-2560/12/6/066020
970   Chiang, A. K. I., Rennie, C. J., Robinson, P. A., Roberts, J. A., Rigozzi, M. K., Whitehouse, R. W.,
971   Hamilton, R. J., & Gordon, E. (2008). Automated characterization of multiple alpha peaks in multi-site
972   electroencephalograms. *Journal of Neuroscience Methods*, *168*(2), 396–411.
973   https://doi.org/10.1016/j.jneumeth.2007.11.001
974   Cohen, M. X. (2014). *Analyzing neural time series data: Theory and practice*. MIT Press.
975   Cohen, M. X. (2017a). Rigor and replication in time-frequency analyses of cognitive electrophysiology
976   data. *International Journal of Psychophysiology*, *111*, 80–87.
977   https://doi.org/10.1016/j.ijpsycho.2016.02.001
978   Cohen, M. X. (2017b). Comparison of linear spatial filters for identifying oscillatory activity in multichannel
979   data. *Journal of Neuroscience Methods*, *278*, 1–12. https://doi.org/10.1016/j.jneumeth.2016.12.016
980   Cohen, M. X. (2017c). Where Does EEG Come From and What Does It Mean? *Trends in Neurosciences*,
981   *40*(4), 208–218. https://doi.org/10.1016/j.tins.2017.02.004
982   Cohen, M. X. (2021). A data-driven method to identify frequency boundaries in multichannel
983   electrophysiology data. *Journal of Neuroscience Methods*, *347*, 108949.
984   https://doi.org/10.1016/j.jneumeth.2020.108949
985   Cohen, M. X., & Gulbinaite, R. (2014). Five methodological challenges in cognitive electrophysiology.
986   *NeuroImage*, *85*, 702–710. https://doi.org/10.1016/j.neuroimage.2013.08.010
987   Cole, S. R., Donoghue, T., Gao, R., & Voytek, B. (2019). NeuroDSP: A package for neural digital signal
988   processing. *Journal of Open Source Software*, *4*(36), 1272. https://doi.org/10.21105/joss.01272
989   Cole, S. R., van der Meij, R., Peterson, E. J., de Hemptinne, C., Starr, P. A., & Voytek, B. (2017).
990   Nonsinusoidal Beta Oscillations Reflect Cortical Pathophysiology in Parkinson's Disease. *The Journal*
991   *of Neuroscience*, *37*(18), 4830–4840. https://doi.org/10.1523/jneurosci.2208-16.2017
992   Cole, S. R., & Voytek, B. (2017). Brain Oscillations and the Importance of Waveform Shape. *Trends in*
993   *Cognitive Sciences*, *21*(2), 137–149. https://doi.org/10.1016/j.tics.2016.12.008
994   Cole, S. R., & Voytek, B. (2018). *Hippocampal theta bursting and waveform shape reflect CA1 spiking*
995   *patterns* [Preprint]. bioRxiv. https://doi.org/10.1101/452987
996   Cole, S. R., & Voytek, B. (2019). Cycle-by-cycle analysis of neural oscillations. *Journal of*
997   *Neurophysiology*, *122*(2), 849–861. https://doi.org/10.1152/jn.00273.2019
998   Corcoran, A. W., Alday, P. M., Schlesewsky, M., & Bornkessel-Schlesewsky, I. (2018). Toward a reliable,
999   automated method of individual alpha frequency (IAF) quantification. *Psychophysiology*, *55*(7),
1000   e13064. https://doi.org/10.1111/psyp.13064
1001   Cross, Z. R., Corcoran, A. W., Schlesewsky, M., Kohler, Mark. J., & Bornkessel-Schlesewsky, I. (2020).
1002   *Oscillatory and aperiodic neural activity jointly predict grammar learning* [Preprint]. bioRxiv.
1003   https://doi.org/10.1101/2020.03.10.984971
1004   Dähne, S., Meinecke, F. C., Haufe, S., Höhne, J., Tangermann, M., Müller, K.-R., & Nikulin, V. V. (2014).
1005   SPoC: A novel framework for relating the amplitude of neuronal oscillations to behaviorally relevant
1006   parameters. *NeuroImage*, *86*, 111–122. https://doi.org/10.1016/j.neuroimage.2013.07.079
1007   de Cheveigné, A., & Arzounian, D. (2018). Robust detrending, rereferencing, outlier detection, and
1008   inpainting for multichannel data. *NeuroImage*, *172*, 903–912.
1009   https://doi.org/10.1016/j.neuroimage.2018.01.035
1010   de Cheveigné, A., & Nelken, I. (2019). Filters: When, Why, and How (Not) to Use Them. *Neuron*, *102*(2),
1011   280–293. https://doi.org/10.1016/j.neuron.2019.02.039
1012   de Cheveigné, A., & Parra, L. C. (2014). Joint decorrelation, a versatile tool for multichannel data
1013   analysis. *NeuroImage*, *98*, 487–505. https://doi.org/10.1016/j.neuroimage.2014.05.068

1014 Donoghue, T., Dominguez, J., & Voytek, B. (2020). Electrophysiological Frequency Band Ratio Measures
1015   Conflate Periodic and Aperiodic Neural Activity. *Eneuro*, ENEURO.0192-20.2020.
1016   https://doi.org/10.1523/ENEURO.0192-20.2020
1017 Donoghue, T., Haller, M., Peterson, E. J., Varma, P., Sebastian, P., Gao, R., Noto, T., Lara, A. H., Wallis,
1018   J. D., Knight, R. T., Shestyuk, A., & Voytek, B. (2020). Parameterizing neural power spectra into
1019   periodic and aperiodic components. *Nature Neuroscience*, *23*(12), 1655–1665.
1020   https://doi.org/10.1038/s41593-020-00744-x
1021 Feingold, J., Gibson, D. J., DePasquale, B., & Graybiel, A. M. (2015). Bursts of beta oscillation
1022   differentiate postperformance activity in the striatum and motor cortex of monkeys performing
1023   movement tasks. *Proceedings of the National Academy of Sciences*, *112*(44), 13687–13692.
1024   https://doi.org/10.1073/pnas.1517629112
1025 Fransen, A. M. M., van Ede, F., & Maris, E. (2015). Identifying neuronal oscillations using rhythmicity.
1026   *NeuroImage*, *118*, 256–267. https://doi.org/10.1016/j.neuroimage.2015.06.003
1027 Frauscher, B., von Ellenrieder, N., Zelmann, R., Doležalová, I., Minotti, L., Olivier, A., Hall, J., Hoffmann,
1028   D., Nguyen, D. K., Kahane, P., Dubeau, F., & Gotman, J. (2018). Atlas of the normal intracranial
1029   electroencephalogram: Neurophysiological awake activity in different cortical areas. *Brain*, *141*(4),
1030   1130–1144. https://doi.org/10.1093/brain/awy035
1031 Freeman, W. J., Holmes, M. D., Burke, B. C., & Vanhatalo, S. (2003). Spatial spectra of scalp EEG and
1032   EMG from awake humans. *Clinical Neurophysiology*, *114*(6), 1053–1068.
1033   https://doi.org/10.1016/S1388-2457(03)00045-2
1034 Freeman, W. J., & Zhai, J. (2009). Simulated power spectral density (PSD) of background
1035   electrocorticogram (ECoG). *Cognitive Neurodynamics*, *3*(1), 97–103. https://doi.org/10.1007/s11571-
1036   008-9064-y
1037 Fries, P. (2005). A mechanism for cognitive dynamics: Neuronal communication through neuronal
1038   coherence. *Trends in Cognitive Sciences*, *9*(10), 474–480. https://doi.org/10.1016/j.tics.2005.08.011
1039 Gao, R., Peterson, E. J., & Voytek, B. (2017). Inferring synaptic excitation/inhibition balance from field
1040   potentials. *NeuroImage*, *158*, 70–78. https://doi.org/10.1016/j.neuroimage.2017.06.078
1041 Gao, R., van den Brink, R. L., Pfeffer, T., & Voytek, B. (2020). Neuronal timescales are functionally
1042   dynamic and shaped by cortical microarchitecture. *ELife*, *9*, e61277.
1043   https://doi.org/10.7554/eLife.61277
1044 Ghosh, M., Shanahan, B. E., Furtak, S. C., Mashour, G. A., Burwell, R. D., & Ahmed, O. J. (2020).
1045   *Instantaneous amplitude and shape of postrhinal theta oscillations differentially encode running
1046   speed* [Preprint]. bioRxiv. https://doi.org/10.1101/2020.06.03.130609
1047 Giehl, J., Noury, N., & Siegel, M. (2021). Dissociating harmonic and non-harmonic phase-amplitude
1048   coupling in the human brain. *NeuroImage*, *227*. https://doi.org/10.1016/j.neuroimage.2020.117648
1049 Gips, B., Bahramisharif, A., Lowet, E., Roberts, M. J., de Weerd, P., Jensen, O., & van der Eerden, J.
1050   (2017). Discovering recurring patterns in electrophysiological recordings. *Journal of Neuroscience
1051   Methods*, *275*, 66–79. https://doi.org/10.1016/j.jneumeth.2016.11.001
1052 Gleeson, P., Davison, A. P., Silver, R. A., & Ascoli, G. A. (2017). A Commitment to Open Source in
1053   Neuroscience. *Neuron*, *96*(5), 964–965. https://doi.org/10.1016/j.neuron.2017.10.013
1054 Gramfort, A. (2013). MEG and EEG data analysis with MNE-Python. *Frontiers in Neuroscience*, 7, 267.
1055   https://doi.org/10.3389/fnins.2013.00267
1056 Grandy, T. H., Werkle-Bergner, M., Chicherio, C., Schmiedek, F., Lövdén, M., & Lindenberger, U. (2013).
1057   Peak individual alpha frequency qualifies as a stable neurophysiological trait marker in healthy
1058   younger and older adults: Alpha stability. *Psychophysiology*, *50*(6), 570–582.
1059   https://doi.org/10.1111/psyp.12043
1060 Grice, J. W., Medellin, E., Jones, I., Horvath, S., McDaniel, H., O'lansen, C., & Baker, M. (2020). Persons
1061   as Effect Sizes. *Advances in Methods and Practices in Psychological Science*, *3*(4), 443–455.
1062   https://doi.org/10.1177/2515245920922982
1063 Groppe, D. M., Bickel, S., Keller, C. J., Jain, S. K., Hwang, S. T., Harden, C., & Mehta, A. D. (2013).
1064   Dominant frequencies of resting human brain activity as measured by the electrocorticogram.
1065   *NeuroImage*, *79*, 223–233. https://doi.org/10.1016/j.neuroimage.2013.04.044
1066 Gross, J. (2014). Analytical methods and experimental approaches for electrophysiological studies of
1067   brain oscillations. *Journal of Neuroscience Methods*, *228*, 57–66.
1068   https://doi.org/10.1016/j.jneumeth.2014.03.007
1069 Gross, J., Baillet, S., Barnes, G. R., Henson, R. N., Hillebrand, A., Jensen, O., Jerbi, K., Litvak, V.,

1070   Maess, B., Oostenveld, R., Parkkonen, L., Taylor, J. R., van Wassenhove, V., Wibral, M., &
1071   Schoffelen, J.-M. (2013). Good practice for conducting and reporting MEG research. *NeuroImage*, *65*,
1072   349–363. https://doi.org/10.1016/j.neuroimage.2012.10.001
1073   Haegens, S., Cousijn, H., Wallis, G., Harrison, P. J., & Nobre, A. C. (2014). Inter- and intra-individual
1074   variability in alpha peak frequency. *NeuroImage*, *92*, 46–55.
1075   https://doi.org/10.1016/j.neuroimage.2014.01.049
1076   Hari, R., & Puce, A. (2017). *MEG-EEG Primer*. Oxford University Press.
1077   Haufe, S., Dähne, S., & Nikulin, V. V. (2014). Dimensionality reduction for the analysis of brain
1078   oscillations. *NeuroImage*, *101*, 583–597. https://doi.org/10.1016/j.neuroimage.2014.06.073
1079   Haufe, S., Meinecke, F., Görgen, K., Dähne, S., Haynes, J.-D., Blankertz, B., & Bießmann, F. (2014). On
1080   the interpretation of weight vectors of linear models in multivariate neuroimaging. *NeuroImage*, *87*,
1081   96–110. https://doi.org/10.1016/j.neuroimage.2013.10.067
1082   Haufe, S., Nikulin, V. V., Müller, K.-R., & Nolte, G. (2013). A critical assessment of connectivity measures
1083   for EEG data: A simulation study. *NeuroImage*, *64*, 120–133.
1084   https://doi.org/10.1016/j.neuroimage.2012.09.036
1085   Hauk, O., Stenroos, M., & Treder, M. (2019). EEG/MEG Source Estimation and Spatial Filtering: The
1086   Linear Toolkit. In S. Supek & C. J. Aine (Eds.), *Magnetoencephalography* (pp. 1–37). Springer
1087   International Publishing. https://doi.org/10.1007/978-3-319-62657-4_85-1
1088   He, B. J. (2014). Scale-free brain activity: Past, present, and future. *Trends in Cognitive Sciences*, *18*(9),
1089   480–487. https://doi.org/10.1016/j.tics.2014.04.003
1090   He, W., Donoghue, T., Sowman, P. F., Seymour, R. A., Brock, J., Crain, S., Voytek, B., & Hillebrand, A.
1091   (2019). *Co-Increasing Neuronal Noise and Beta Power in the Developing Brain* (p. 49) [Preprint].
1092   bioRxiv. https://doi.org/10.1101/839258
1093   Hindriks, R., Micheli, C., Mantini, D., & Deco, G. (2017). *Human Resting-State Electrophysiological
1094   Networks In The Alpha Frequency Band: Evidence From Magnetoencephalographic Source Imaging*
1095   (p.) [Preprint]. bioRxiv. https://doi.org/10.1101/142091
1096   Holdgraf, C., Appelhoff, S., Bickel, S., Bouchard, K., D'Ambrosio, S., David, O., Devinsky, O., Dichter, B.,
1097   Flinker, A., Foster, B. L., Gorgolewski, K. J., Groen, I., Groppe, D., Gunduz, A., Hamilton, L., Honey,
1098   C. J., Jas, M., Knight, R., Lachaux, J.-P., … Hermes, D. (2019). IEEG-BIDS, extending the Brain
1099   Imaging Data Structure specification to human intracranial electrophysiology. *Scientific Data*, *6*(1),
1100   102. https://doi.org/10.1038/s41597-019-0105-7
1101   Huang, Y., Parra, L. C., & Haufe, S. (2016). The New York Head—A precise standardized volume
1102   conductor model for EEG source localization and tES targeting. *NeuroImage*, *140*, 150–162.
1103   https://doi.org/10.1016/j.neuroimage.2015.12.019
1104   Hyvärinen, A., & Oja, E. (2000). Independent component analysis: Algorithms and applications. *Neural
1105   Networks*, *13*(4–5), 411–430. https://doi.org/10.1016/S0893-6080(00)00026-5
1106   Jas, M., & Dupré, T. (2017). Learning the Morphology of Brain Signals Using Alpha-Stable Convolutional
1107   Sparse Coding. *Advances in Neural Information Processing Systems*, 1099–1108.
1108   Jas, M., Engemann, D. A., Bekhti, Y., Raimondo, F., & Gramfort, A. (2017). Autoreject: Automated artifact
1109   rejection for MEG and EEG data. *NeuroImage*, *159*, 417–429.
1110   https://doi.org/10.1016/j.neuroimage.2017.06.030
1111   Jas, M., Larson, E., Engemann, D. A., Leppäkangas, J., Taulu, S., Hämäläinen, M., & Gramfort, A.
1112   (2018). A Reproducible MEG/EEG Group Study With the MNE Software: Recommendations, Quality
1113   Assessments, and Good Practices. *Frontiers in Neuroscience*, *12*, 530.
1114   https://doi.org/10.3389/fnins.2018.00530
1115   Jones, S. R. (2016). When brain rhythms aren't 'rhythmic': Implication for their mechanisms and meaning.
1116   *Current Opinion in Neurobiology*, *40*, 72–80. https://doi.org/10.1016/j.conb.2016.06.010
1117   Kathawalla, U.-K., Silverstein, P., & Syed, M. (2020). *Easing Into Open Science: A Tutorial for Graduate
1118   Students* [Preprint]. PsyArXiv. https://doi.org/10.31234/osf.io/vzjdp
1119   Keil, A., Debener, S., Gratton, G., Junghöfer, M., Kappenman, E. S., Luck, S. J., Luu, P., Miller, G. A., &
1120   Yee, C. M. (2014). Committee report: Publication guidelines and recommendations for studies using
1121   electroencephalography and magnetoencephalography: Guidelines for EEG and MEG.
1122   *Psychophysiology*, *51*(1), 1–21. https://doi.org/10.1111/psyp.12147
1123   Kiebel, S. J., Tallon-Baudry, C., & Friston, K. J. (2005). Parametric analysis of oscillatory activity as
1124   measured with EEG/MEG. *Human Brain Mapping*, *26*(3), 170–177.
1125   https://doi.org/10.1002/hbm.20153

1126   Klimesch, W. (1999). EEG alpha and theta oscillations reflect cognitive and memory performance: A
1127   review and analysis. *Brain Research Reviews*, *29*(2), 169–195. https://doi.org/10.1016/S0165-
1128   0173(98)00056-3
1129   Koles, Z. J. (1991). The quantitative extraction and topographic mapping of the abnormal components in
1130   the clinical EEG. *Electroencephalography and Clinical Neurophysiology*, *79*(6), 440–447.
1131   https://doi.org/10.1016/0013-4694(91)90163-X
1132   Kosciessa, J. Q., Grandy, T. H., Garrett, D. D., & Werkle-Bergner, M. (2020). Single-trial characterization
1133   of neural rhythms: Potential and challenges. *NeuroImage*, *206*, 116331.
1134   https://doi.org/10.1016/j.neuroimage.2019.116331
1135   Kramer, M. A., Tort, A. B. L., & Kopell, N. J. (2008). Sharp edge artifacts and spurious coupling in EEG
1136   frequency comodulation measures. *Journal of Neuroscience Methods*, *170*(2), 352–357.
1137   https://doi.org/10.1016/j.jneumeth.2008.01.020
1138   Krol, L. R., Pawlitzki, J., Lotte, F., Gramann, K., & Zander, T. O. (2018). SEREEGA: Simulating event-
1139   related EEG activity. *Journal of Neuroscience Methods*, *309*, 13–24.
1140   https://doi.org/10.1016/j.jneumeth.2018.08.001
1141   Lachaux, J.-P., Rodriguez, E., Martinerie, J., Varela, F. J., & others. (1999). Measuring phase synchrony
1142   in brain signals. *Human Brain Mapping*, *8*(4), 194–208. https://doi.org/10.1002/(SICI)1097-
1143   0193(1999)8:4<194::AID-HBM4>3.0.CO;2-C
1144   Lansbergen, M. M., Arns, M., van Dongen-Boomsma, M., Spronk, D., & Buitelaar, J. K. (2011). The
1145   increase in theta/beta ratio on resting-state EEG in boys with attention-deficit/hyperactivity disorder is
1146   mediated by slow alpha peak frequency. *Progress in Neuro-Psychopharmacology and Biological
1147   Psychiatry*, *35*(1), 47–52. https://doi.org/10.1016/j.pnpbp.2010.08.004
1148   Lendner, J. D., Helfrich, R. F., Mander, B. A., Romundstad, L., Lin, J. J., Walker, M. P., Larsson, P. G., &
1149   Knight, R. T. (2020). An electrophysiological marker of arousal level in humans. *ELife*, *9*, e55092.
1150   https://doi.org/10.7554/eLife.55092
1151   Lepage, K. Q., Kramer, M. A., & Eden, U. T. (2013). Some Sampling Properties of Common Phase
1152   Estimators. *Neural Computation*, *25*(4), 901–921.
1153   Lindsley, D. B. (1939). A Longitudinal Study of the Occipital Alpha Rhythm in Normal Children: Frequency
1154   and Amplitude Standards. *The Pedagogical Seminary and Journal of Genetic Psychology*, *55*(1),
1155   197–213. https://doi.org/10.1080/08856559.1939.10533190
1156   Lopes da Silva, F. (2013). EEG and MEG: Relevance to Neuroscience. *Neuron*, *80*(5), 1112–1128.
1157   https://doi.org/10.1016/j.neuron.2013.10.017
1158   Lotte, F. & Cuntai Guan. (2011). Regularizing Common Spatial Patterns to Improve BCI Designs: Unified
1159   Theory and New Algorithms. *IEEE Transactions on Biomedical Engineering*, *58*(2), 355–362.
1160   https://doi.org/10.1109/TBME.2010.2082539
1161   Lozano-Soldevilla, D., ter Huurne, N., & Oostenveld, R. (2016). Neuronal Oscillations with Non-sinusoidal
1162   Morphology Produce Spurious Phase-to-Amplitude Coupling and Directionality. *Frontiers in
1163   Computational Neuroscience*, *10*. https://doi.org/10.3389/fncom.2016.00087
1164   Lundqvist, M., Rose, J., Herman, P., Brincat, S. L., Buschman, T. J., & Miller, E. K. (2016). Gamma and
1165   Beta Bursts Underlie Working Memory. *Neuron*, *90*(1), 152–164.
1166   https://doi.org/10.1016/j.neuron.2016.02.028
1167   Mahjoory, K., Nikulin, V. V., Botrel, L., Linkenkaer-Hansen, K., Fato, M. M., & Haufe, S. (2017).
1168   Consistency of EEG source localization and connectivity estimates. *NeuroImage*, *152*, 590–601.
1169   https://doi.org/10.1016/j.neuroimage.2017.02.076
1170   Mahjoory, K., Schoffelen, J.-M., Keitel, A., & Gross, J. (2020). The frequency gradient of human resting-
1171   state brain oscillations follows cortical hierarchies. *ELife*, *9*, e53715.
1172   https://doi.org/10.7554/eLife.53715
1173   Maris, E. (2012). Statistical testing in electrophysiological studies: Statistical testing in electrophysiological
1174   studies. *Psychophysiology*, *49*(4), 549–565. https://doi.org/10.1111/j.1469-8986.2011.01320.x
1175   Maris, E., & Oostenveld, R. (2007). Nonparametric statistical testing of EEG- and MEG-data. *Journal of
1176   Neuroscience Methods*, *164*(1), 177–190. https://doi.org/10.1016/j.jneumeth.2007.03.024
1177   Mazaheri, A., Slagter, H. A., Thut, G., & Foxe, J. J. (2018). Orchestration of brain oscillations: Principles
1178   and functions. *European Journal of Neuroscience*, *48*(7), 2385–2388.
1179   https://doi.org/10.1111/ejn.14189
1180   Miller, E. K., Lundqvist, M., & Bastos, A. M. (2018). Working Memory 2.0. *Neuron*, *100*(2), 463–475.
1181   https://doi.org/10.1016/j.neuron.2018.09.023

1182 Miller, K. J., Honey, C. J., Hermes, D., Rao, R. P., den Nijs, M., & Ojemann, J. G. (2014). Broadband
1183   changes in the cortical surface potential track activation of functionally diverse neuronal populations.
1184   *NeuroImage*, *85*, 711–720. https://doi.org/10.1016/j.neuroimage.2013.08.070
1185 Miller, K. J., Sorensen, L. B., Ojemann, J. G., & den Nijs, M. (2009). Power-Law Scaling in the Brain
1186   Surface Electric Potential. *PLOS Computational Biology*, *5*(12), e1000609.
1187   https://doi.org/10.1371/journal.pcbi.1000609
1188 Mortezapouraghdam, Z., Corona-Strauss, F. I., Takahashi, K., & Strauss, D. J. (2018). Reducing the
1189   Effect of Spurious Phase Variations in Neural Oscillatory Signals. *Frontiers in Computational
1190   Neuroscience*, *12*, 82. https://doi.org/10.3389/fncom.2018.00082
1191 Muthukumaraswamy, S. D., & Singh, K. D. (2011). A cautionary note on the interpretation of phase-
1192   locking estimates with concurrent changes in power. *Clinical Neurophysiology*, *122*(11), 2324–2325.
1193   https://doi.org/10.1016/j.clinph.2011.04.003
1194 Newson, J. J., & Thiagarajan, T. C. (2019). EEG Frequency Bands in Psychiatric Disorders: A Review of
1195   Resting State Studies. *Frontiers in Human Neuroscience*, *12*.
1196   https://doi.org/10.3389/fnhum.2018.00521
1197 Neymotin, S. A., Barczak, A., O'Connell, M. N., McGinnis, T., Markowitz, N., Espinal, E., Griffith, E.,
1198   Anwar, H., Dura-Bernal, S., Lytton, W. W., Jones, S. R., Bickel, S., & Lakatos, P. (2020). *Taxonomy
1199   of neural oscillation events in primate auditory cortex* [Preprint]. bioRxiv.
1200   https://doi.org/10.1101/2020.04.16.045021
1201 Neymotin, S. A., Daniels, D. S., Caldwell, B., McDougal, R. A., Carnevale, N. T., Jas, M., Moore, C. I.,
1202   Hines, M. L., Hämäläinen, M., & Jones, S. R. (2020). Human Neocortical Neurosolver (HNN), a new
1203   software tool for interpreting the cellular and network origin of human MEG/EEG data. *ELife*, *9*,
1204   e51214. https://doi.org/10.7554/eLife.51214
1205 Nikulin, V. V., Nolte, G., & Curio, G. (2011). A novel method for reliable and fast extraction of neuronal
1206   EEG/MEG oscillations on the basis of spatio-spectral decomposition. *NeuroImage*, *55*(4), 1528–1535.
1207   https://doi.org/10.1016/j.neuroimage.2011.01.057
1208 Niso, G., Gorgolewski, K. J., Bock, E., Brooks, T. L., Flandin, G., Gramfort, A., Henson, R. N., Jas, M.,
1209   Litvak, V., T. Moreau, J., Oostenveld, R., Schoffelen, J.-M., Tadel, F., Wexler, J., & Baillet, S. (2018).
1210   MEG-BIDS, the brain imaging data structure extended to magnetoencephalography. *Scientific Data*,
1211   *5*(1), 180110. https://doi.org/10.1038/sdata.2018.110
1212 Nunez, P. L., & Srinivasan, R. (2006). *Electric fields of the brain: The neurophysics of EEG* (2nd ed).
1213   Oxford University Press.
1214 O'Neill, G. C., Tewarie, P., Vidaurre, D., Liuzzi, L., Woolrich, M. W., & Brookes, M. J. (2018). Dynamics of
1215   large-scale electrophysiological networks: A technical review. *NeuroImage*, *180*, 559–576.
1216   https://doi.org/10.1016/j.neuroimage.2017.10.003
1217 Oostenveld, R., Fries, P., Maris, E., & Schoffelen, J.-M. (2011). FieldTrip: Open Source Software for
1218   Advanced Analysis of MEG, EEG, and Invasive Electrophysiological Data. *Computational Intelligence
1219   and Neuroscience*, *2011*, 1–9. https://doi.org/10.1155/2011/156869
1220 Palva, J. M., Wang, S. H., Palva, S., Zhigalov, A., Monto, S., Brookes, M. J., Schoffelen, J.-M., & Jerbi, K.
1221   (2018). Ghost interactions in MEG/EEG source space: A note of caution on inter-areal coupling
1222   measures. *NeuroImage*, *173*, 632–643. https://doi.org/10.1016/j.neuroimage.2018.02.032
1223 Palva, S., & Palva, J. M. (2012). Discovering oscillatory interaction networks with M/EEG: Challenges and
1224   breakthroughs. *Trends in Cognitive Sciences*, *16*(4), 219–230.
1225   https://doi.org/10.1016/j.tics.2012.02.004
1226 Parra, L. C., Spence, C. D., Gerson, A. D., & Sajda, P. (2005). Recipes for the linear analysis of EEG.
1227   *NeuroImage*, *28*(2), 326–341. https://doi.org/10.1016/j.neuroimage.2005.05.032
1228 Pascual-marqui, R. D., Valdes-sosa, P. A., & Alvarez-amador, A. (1988). A Parametric Model for
1229   Multichannel EEG Spectra. *International Journal of Neuroscience*, *40*(1–2), 89–99.
1230   https://doi.org/10.3109/00207458808985730
1231 Pernet, C. R., Appelhoff, S., Gorgolewski, K. J., Flandin, G., Phillips, C., Delorme, A., & Oostenveld, R.
1232   (2019). EEG-BIDS, an extension to the brain imaging data structure for electroencephalography.
1233   *Scientific Data*, *6*(1), 103. https://doi.org/10.1038/s41597-019-0104-8
1234 Pernet, C. R., Garrido, M. I., Gramfort, A., Maurits, N., Michel, C. M., Pang, E., Salmelin, R., Schoffelen,
1235   J. M., Valdes-Sosa, P. A., & Puce, A. (2020). Issues and recommendations from the OHBM
1236   COBIDAS MEEG committee for reproducible EEG and MEG research. *Nature Neuroscience*, *23*(12),
1237   1473–1483. https://doi.org/10.1038/s41593-020-00709-0

Pesaran, B., Vinck, M., Einevoll, G. T., Sirota, A., Fries, P., Siegel, M., Truccolo, W., Schroeder, C. E., & Srinivasan, R. (2018). Investigating large-scale brain dynamics using field potential recordings: Analysis and interpretation. *Nature Neuroscience*. https://doi.org/10.1038/s41593-018-0171-8

Pfurtscheller, G., & Lopes da Silva, F. H. (1999). Event-related EEG/MEG synchronization and desynchronization: Basic principles. *Clinical Neurophysiology*, *110*(11), 1842–1857. https://doi.org/10.1016/S1388-2457(99)00141-8

Piastra, M. C., Nüßing, A., Vorwerk, J., Clerc, M., Engwer, C., & Wolters, C. H. (2020). A comprehensive study on electroencephalography and magnetoencephalography sensitivity to cortical and subcortical sources. *Human Brain Mapping*, hbm.25272. https://doi.org/10.1002/hbm.25272

Podvalny, E., Noy, N., Harel, M., Bickel, S., Chechik, G., Schroeder, C. E., Mehta, A. D., Tsodyks, M., & Malach, R. (2015). A unifying principle underlying the extracellular field potential spectral responses in the human cortex. *Journal of Neurophysiology*, *114*(1), 505–519. https://doi.org/10.1152/jn.00943.2014

Popov, T., Oostenveld, R., & Schoffelen, J. M. (2018). FieldTrip Made Easy: An Analysis Protocol for Group Analysis of the Auditory Steady State Brain Response in Time, Frequency, and Space. *Frontiers in Neuroscience*, *12*, 711. https://doi.org/10.3389/fnins.2018.00711

Quinn, A. J., van Ede, F., Brookes, M. J., Heideman, S. G., Nowak, M., Seedat, Z. A., Vidaurre, D., Zich, C., Nobre, A. C., & Woolrich, M. W. (2019). Unpacking Transient Event Dynamics in Electrophysiological Power Spectra. *Brain Topography*, *32*, 1020–1034. https://doi.org/10.1007/s10548-019-00745-5

Robertson, M. M., Furlong, S., Voytek, B., Donoghue, T., Boettiger, C. A., & Sheridan, M. A. (2019). EEG Power Spectral Slope differs by ADHD status and stimulant medication exposure in early childhood. *Journal of Neurophysiology*, *122*(6), 2427–2437. https://doi.org/10.1152/jn.00388.2019

Sameni, R., & Seraj, E. (2017). A robust statistical framework for instantaneous electroencephalogram phase and frequency estimation and analysis. *Physiological Measurement*, *38*(12), 2141–2163. https://doi.org/10.1088/1361-6579/aa93a1

Sanz Leon, P., Knock, S. A., Woodman, M. M., Domide, L., Mersmann, J., McIntosh, A. R., & Jirsa, V. (2013). The Virtual Brain: A simulator of primate brain network dynamics. *Frontiers in Neuroinformatics*, *7*. https://doi.org/10.3389/fninf.2013.00010

Schaworonkow, N., Blythe, D. A. J., Kegeles, J., Curio, G., & Nikulin, V. V. (2015). Power-law dynamics in neuronal and behavioral data introduce spurious correlations: Power-Law Dynamics in Neuronal and Behavioral Data. *Human Brain Mapping*, *36*(8), 2901–2914. https://doi.org/10.1002/hbm.22816

Schaworonkow, N., & Nikulin, V. V. (2019). Spatial neuronal synchronization and the waveform of oscillations: Implications for EEG and MEG. *PLOS Computational Biology*, *15*(5), e1007055. https://doi.org/10.1371/journal.pcbi.1007055

Schoffelen, J.-M., & Gross, J. (2009). Source connectivity analysis with MEG and EEG. *Human Brain Mapping*, *30*(6), 1857–1865. https://doi.org/10.1002/hbm.20745

Sherman, M. A., Lee, S., Law, R., Haegens, S., Thorn, C. A., Hamalainen, M. S., Moore, C. I., & Jones, S. R. (2016). Neural mechanisms of transient neocortical beta rhythms: Converging evidence from humans, computational modeling, monkeys, and mice. *Proceedings of the National Academy of Sciences*, *113*(33), E4885–E4894. https://doi.org/10.1073/pnas.1604135113

Shin, H., Law, R., Tsutsui, S., Moore, C. I., & Jones, S. R. (2017). The rate of transient beta frequency events predicts behavior across tasks and species. *ELife*, *6*, e29086. https://doi.org/10.7554/eLife.29086

Stokes, M., & Spaak, E. (2016). The Importance of Single-Trial Analyses in Cognitive Neuroscience. *Trends in Cognitive Sciences*, *20*(7), 483–486. https://doi.org/10.1016/j.tics.2016.05.008

Timmer, J., & Konig, M. (1995). On Generating Power Law Noise. *Astronomy and Astrophysics*, *300*, 707–710.

Urigüen, J. A., & Garcia-Zapirain, B. (2015). EEG artifact removal—State-of-the-art and guidelines. *Journal of Neural Engineering*, *12*(3), 031001. https://doi.org/10.1088/1741-2560/12/3/031001

van Ede, F., Quinn, A. J., Woolrich, M. W., & Nobre, A. C. (2018). Neural Oscillations: Sustained Rhythms or Transient Burst-Events? *Trends in Neurosciences*, *41*(7), 415–417. https://doi.org/10.1016/j.tins.2018.04.004

van Vugt, M. K., Sederberg, P. B., & Kahana, M. J. (2007). Comparison of spectral analysis methods for characterizing brain oscillations. *Journal of Neuroscience Methods*, *162*(1–2), 49–63. https://doi.org/10.1016/j.jneumeth.2006.12.004

Oscillation Methods

1294 VanRullen, R. (2016). Perceptual Cycles. *Trends in Cognitive Sciences*, *20*(10), 723–735.
1295   https://doi.org/10.1016/j.tics.2016.07.006
1296 Varela, F. J., Lachaux, J.-P., Rodriguez, E., & Martinerie, J. (2001). The brainweb: Phase synchronization
1297   and large-scale integration. *Nature Reviews Neuroscience*, *2*(4), 229–239.
1298   https://doi.org/10.1038/35067550
1299 Vaz, A. P., Yaffe, R. B., Wittig, J. H., Inati, S. K., & Zaghloul, K. A. (2017). Dual origins of measured
1300   phase-amplitude coupling reveal distinct neural mechanisms underlying episodic memory in the
1301   human cortex. *NeuroImage*, *148*, 148–159. https://doi.org/10.1016/j.neuroimage.2017.01.001
1302 Vidaurre, D., Quinn, A. J., Baker, A. P., Dupret, D., Tejero-Cantero, A., & Woolrich, M. W. (2016).
1303   Spectrally resolved fast transient brain states in electrophysiological data. *NeuroImage*, *126*, 81–95.
1304   https://doi.org/10.1016/j.neuroimage.2015.11.047
1305 Voytek, B. (2016). The Virtuous Cycle of a Data Ecosystem. *PLOS Computational Biology*, *12*(8),
1306   e1005037. https://doi.org/10.1371/journal.pcbi.1005037
1307 Voytek, B., & Knight, R. T. (2015). Dynamic Network Communication as a Unifying Neural Basis for
1308   Cognition, Development, Aging, and Disease. *Biological Psychiatry*, *77*(12), 1089–1097.
1309   https://doi.org/10.1016/j.biopsych.2015.04.016
1310 Voytek, B., Kramer, M. A., Case, J., Lepage, K. Q., Tempesta, Z. R., Knight, R. T., & Gazzaley, A. (2015).
1311   Age-Related Changes in 1/f Neural Electrophysiological Noise. *Journal of Neuroscience*, *35*(38),
1312   13257–13265. https://doi.org/10.1523/JNEUROSCI.2332-14.2015
1313 Wacker, M., & Witte, H. (2013). Time-frequency Techniques in Biomedical Signal Analysis: A Tutorial
1314   Review of Similarities and Differences. *Methods of Information in Medicine*, *52*(04), 279–296.
1315   https://doi.org/10.3414/ME12-01-0083
1316 Wang, X.-J. (2010). Neurophysiological and Computational Principles of Cortical Rhythms in Cognition.
1317   *Physiological Reviews*, *90*(3), 1195–1268. https://doi.org/10.1152/physrev.00035.2008
1318 Waschke, L., Donoghue, T., Fiedler, L., Smith, S., Voytek, B., & Obleser, J. (2021). *Modality-specific
1319   tracking of attention and sensory statistics in the human electrophysiological spectral exponent*
1320   [Preprint]. bioRxiv. https://doi.org/10.1101/2021.01.13.426522
1321 Watrous, A. J., & Buchanan, R. J. (2020). The Oscillatory ReConstruction Algorithm adaptively identifies
1322   frequency bands to improve spectral decomposition in human and rodent neural recordings. *Journal
1323   of Neurophysiology*, *124*(6), 1914–1922. https://doi.org/10.1152/jn.00292.2020
1324 Wen, H., & Liu, Z. (2016). Separating Fractal and Oscillatory Components in the Power Spectrum of
1325   Neurophysiological Signal. *Brain Topography*, *29*(1), 13–26. https://doi.org/10.1007/s10548-015-
1326   0448-0
1327 Wessel, J. R. (2020). β-Bursts Reveal the Trial-to-Trial Dynamics of Movement Initiation and
1328   Cancellation. *The Journal of Neuroscience*, *40*(2), 411–423.
1329   https://doi.org/10.1523/JNEUROSCI.1887-19.2019
1330 Whitten, T. A., Hughes, A. M., Dickson, C. T., & Caplan, J. B. (2011). A better oscillation detection
1331   method robustly extracts EEG rhythms across brain state changes: The human alpha rhythm as a
1332   test case. *NeuroImage*, *54*(2), 860–874. https://doi.org/10.1016/j.neuroimage.2010.08.064
1333 Widmann, A., Schröger, E., & Maess, B. (2015). Digital filter design for electrophysiological data – a
1334   practical approach. *Journal of Neuroscience Methods*, *250*, 34–46.
1335   https://doi.org/10.1016/j.jneumeth.2014.08.002
1336 Wilson, G., Bryan, J., Cranston, K., Kitzes, J., Nederbragt, L., & Teal, T. K. (2017). Good enough
1337   practices in scientific computing. *PLOS Computational Biology*, *13*(6), e1005510.
1338   https://doi.org/10.1371/journal.pcbi.1005510
1339 Wutz, A., Melcher, D., & Samaha, J. (2018). Frequency modulation of neural oscillations according to
1340   visual task demands. *Proceedings of the National Academy of Sciences*, *115*(6), 1346–1351.
1341   https://doi.org/10.1073/pnas.1713318115
1342 Zich, C., Quinn, A. J., Mardell, L. C., Ward, N. S., & Bestmann, S. (2020). Dissecting Transient Burst
1343   Events. *Trends in Cognitive Sciences*, *24*(10), 784–788. https://doi.org/10.1016/j.tics.2020.07.004
1344

1345 **Box 1**: Overview of methodological considerations for measuring neural oscillations
1346

| Data Properties	Methodological Issues	Recommendation
neural oscillations are variably present, and may not be present in the recording	if there are no oscillations, applied measures won't reflect oscillatory activity, but will return a value reflecting aperiodic activity	verify the presence of an oscillation, such as with spectral peak detection or with burst detection in the time domain
neural oscillations have variable peak frequencies	measures applied using canonically defined frequency bands may fail to accurately capture oscillatory activity	verify frequency ranges and individualize as needed
neural oscillations co-exist with dynamic aperiodic activity	measured variation may arise due to changes in aperiodic activity, rather than changes in oscillations	measure and control for changes in aperiodic neural activity, evaluating whether it explains measured changes
neural oscillations are variable across time, exhibiting burst-like properties	burst properties may be conflated when analyzing spectral power, and trial averages may suggest illusory sustained activity	examine single trial data for temporal variation, and use burst detection to evaluate burst properties
neural oscillations have non-sinusoidal waveform shape	analysis methods often assume sinusoidal structure, and may return spurious results in the case of non-sinusoidal oscillations	examine waveform shape measures to evaluate if waveform shape may underlie the results
multiple neural oscillations co-exist across the brain, and may overlap across space	multiple distinct sources may create destructive interference, in which case measures won't accurately reflect underlying activity	apply source separation techniques in order to reduce overlap of different types of oscillations
neural oscillations have variable signal-to-noise ratio	without adequate signal to noise ratio, measures may be unreliable or inaccurate	evaluate the required signal-to-noise ratio, and potential ways to optimize it for all applied measures

1347
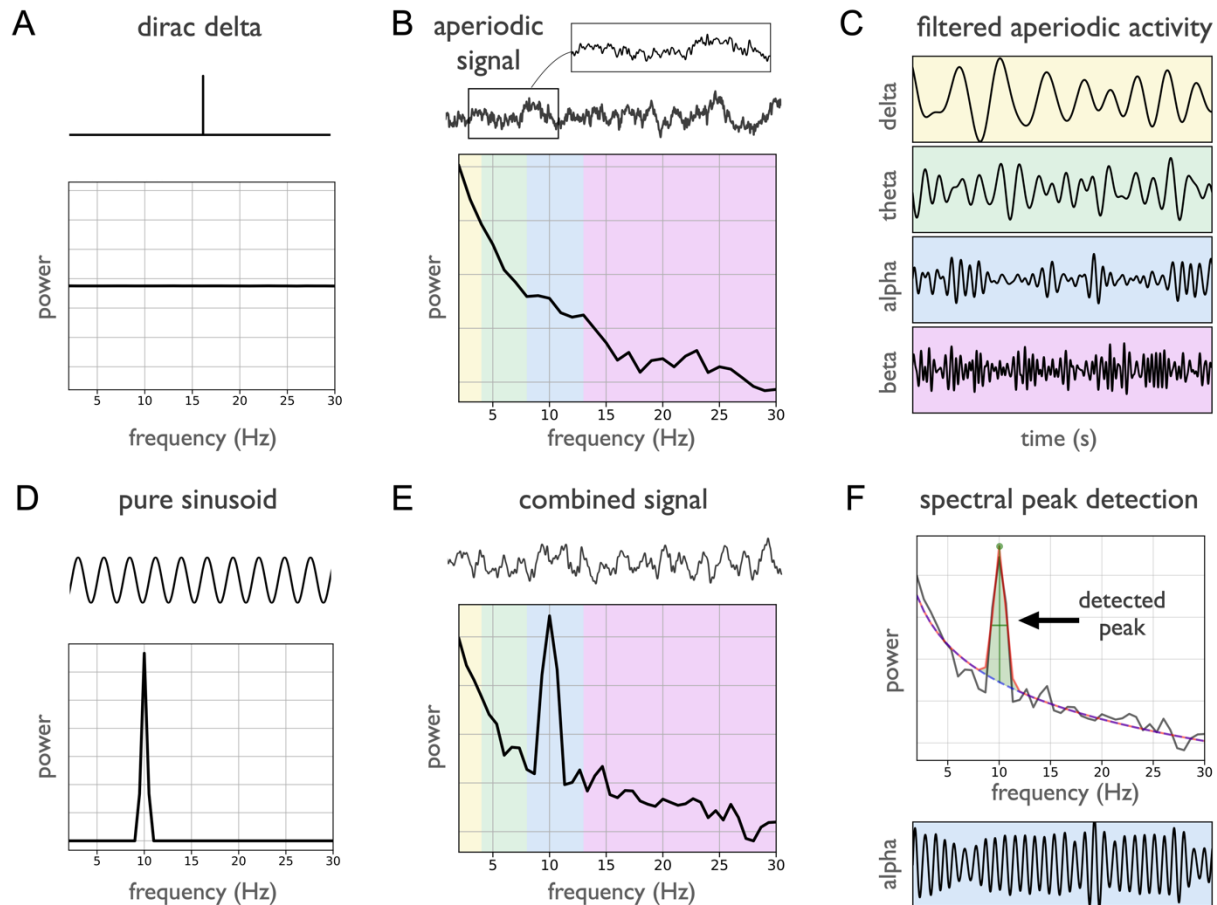
1348
1349 **Figure 1: Without verified oscillatory activity, applied measures may reflect aperiodic activity. A**)
1350 Non-oscillatory signals such as the dirac delta function exhibit power across all frequencies. **B**) Similarly, a
1351 non-oscillatory 1/f signal also has power across all frequencies, including canonical narrowband regions:
1352 delta (yellow), theta (green), alpha (blue), and beta (purple). This power spectrum illustrates the fact that
1353 just because there is power at a frequency, that does not imply there is a dominant oscillation at that
1354 frequency. **C**) Narrowband filtered traces of the signal shown in B, that appear to be rhythmic. Note that
1355 this reflects band-power from the aperiodic activity, rather than any narrowband oscillation. **D**) Rhythmic
1356 signals, such as a pure sinusoid, exhibit as a dominant peak in the power spectrum. **E**) A combined signal
1357 that contains aperiodic activity and a narrowband alpha oscillation. In this case, the oscillation is visible as
1358 a peak in the power spectrum above the spectral contribution from the aperiodic 1/f-like signal. **F**) Spectral
1359 peaks can be detected in order to identify putative oscillations in the data, as shown by the identified peak,
1360 in green. Spectral peak detection can be used to select frequency bands for further analysis, for example
1361 selecting the alpha range to be filtered for subsequent analysis (bottom).
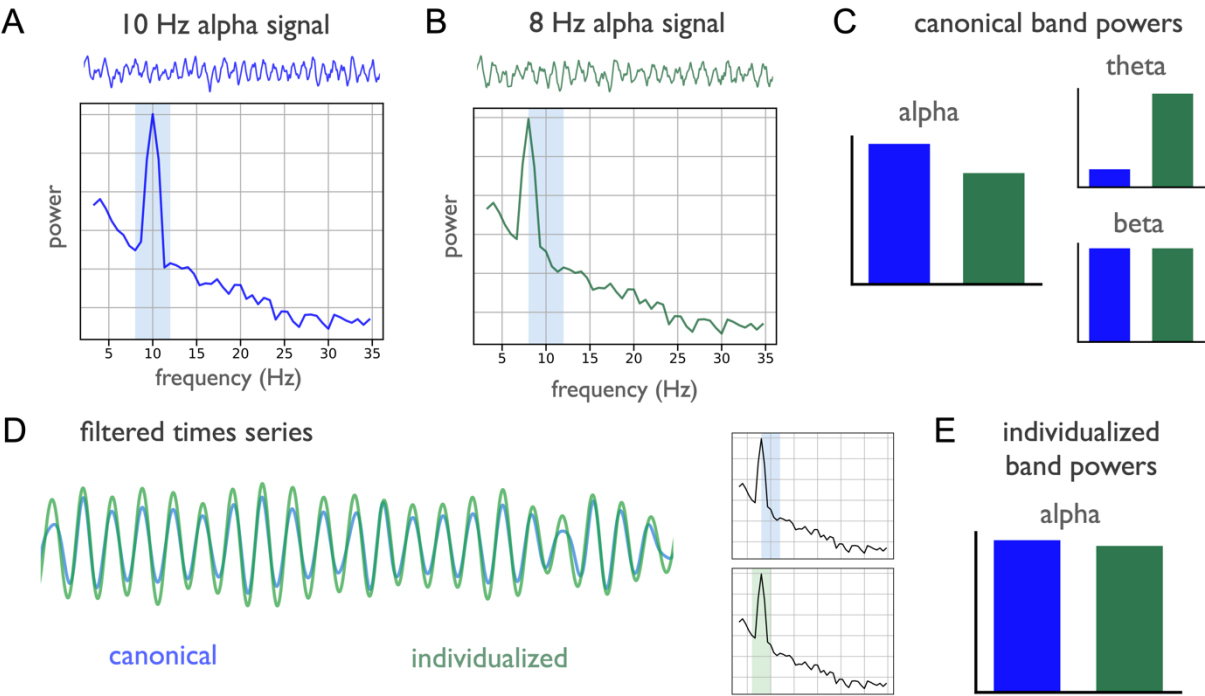1362

1363

1364 **Figure 2: Canonical frequency band ranges may fail to capture narrowband peaks. A**) A simulated
1365 signal, and corresponding power spectrum, with a prominent 10 Hz alpha oscillation. Shaded in blue is the
1366 canonical alpha range (8-12 Hz). **B**) Another signal with a prominent alpha oscillation, with a peak frequency
1367 of 8 Hz. **C**) Using canonical bands ranges, the amount of alpha power is found to be significantly differently
1368 between the signals from A & B. When examining adjacent frequency bands, (right), there is also a
1369 measured difference in theta power, due to the alpha peak drifting into the canonical theta range. These
1370 results suggest differences in oscillatory power between signals, however this is actually driven by a
1371 difference in alpha peak frequency. **D**) The time series from B, filtered into the alpha frequency range, using
1372 both the canonical range (blue) and an individualized range (green). The individualized range is tuned to
1373 the peak frequency of the time series (see inset power spectra). Note that the individualized filter captures
1374 more narrowband activity. **E**) Using individualized frequency bands, a difference in measured alpha power
1375 is no longer seen, consistent with the measured difference in C being due to a mismatch in peak frequency.
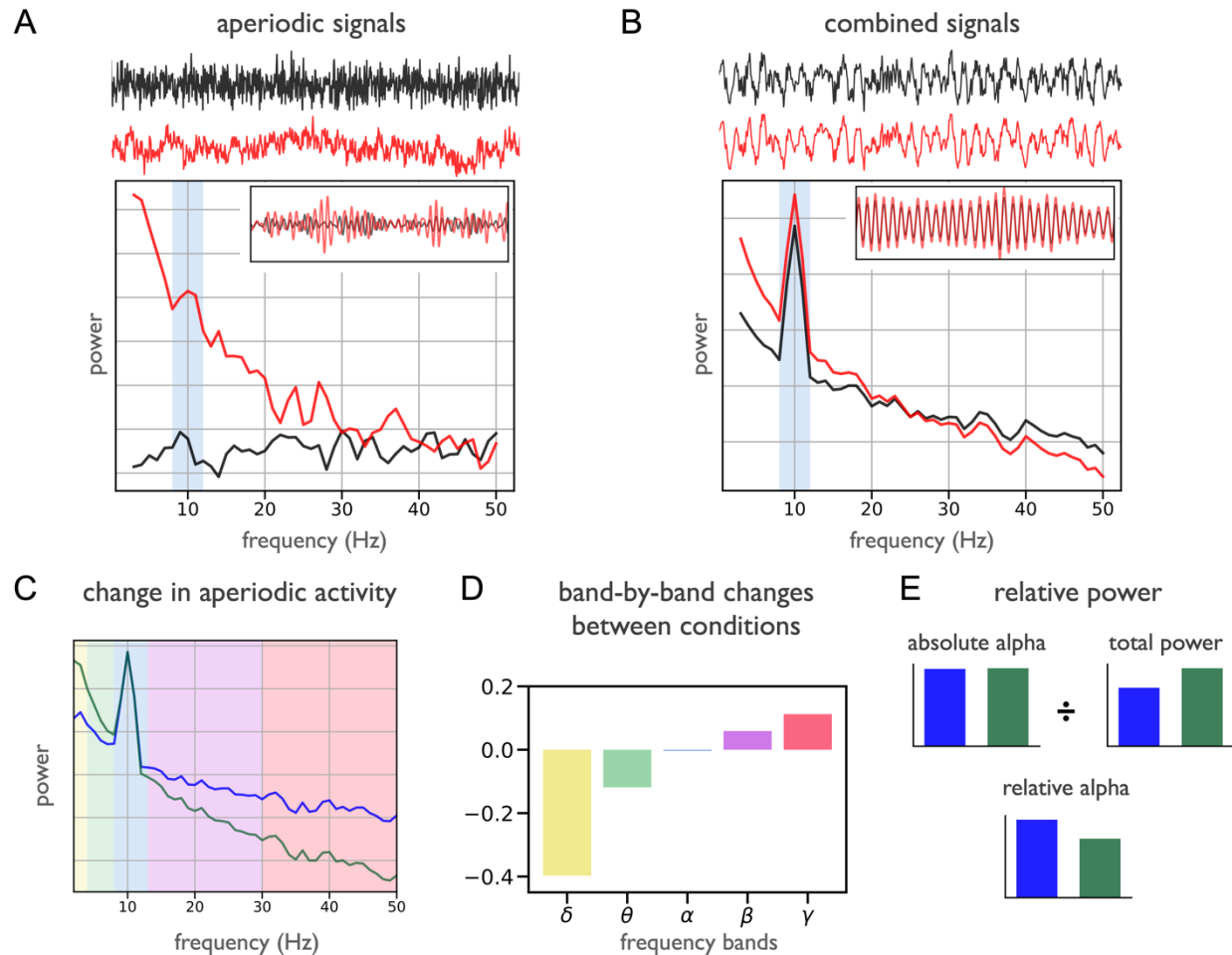
1376

Figure 3: Variations in aperiodic activity influence band-power measures. A) Examples of aperiodic white (black) and pink (red) noise signals that display different patterns of power across frequencies, as seen in their power spectra. Shaded in blue is the canonical alpha range, with time-series filtered in the alpha-range shown in the inset. Note that the pink noise signal appears to have increased 'alpha' power. **B**) Simulated combined signals containing both aperiodic and oscillatory power (black), and with a change in the aperiodic component (red), after being rotated in the spectral domain. Note that in A & B, what appears to be band-specific changes actually reflect differences in aperiodic activity. **C**) A comparison between power spectra for combined signals simulated with the same oscillatory component with different aperiodic activity. Shading reflects different frequency bands, including delta (yellow), theta (green), alpha (blue), beta (purple) and gamma (red). **D**) Absolute differences in power, calculated separately for each frequency band, for the spectra in C. Note that despite the difference in the data being simulated as a change in the aperiodic component, a band-by-band analysis suggests a pattern of changes across distinct frequency bands. **E**) Relative alpha power (bottom) is calculated as absolute band power (top left), divided by the total power (top right). Note that despite no difference in the amount of alpha power, there is measured change in relative power, due to systematically different aperiodic activity between the signals.
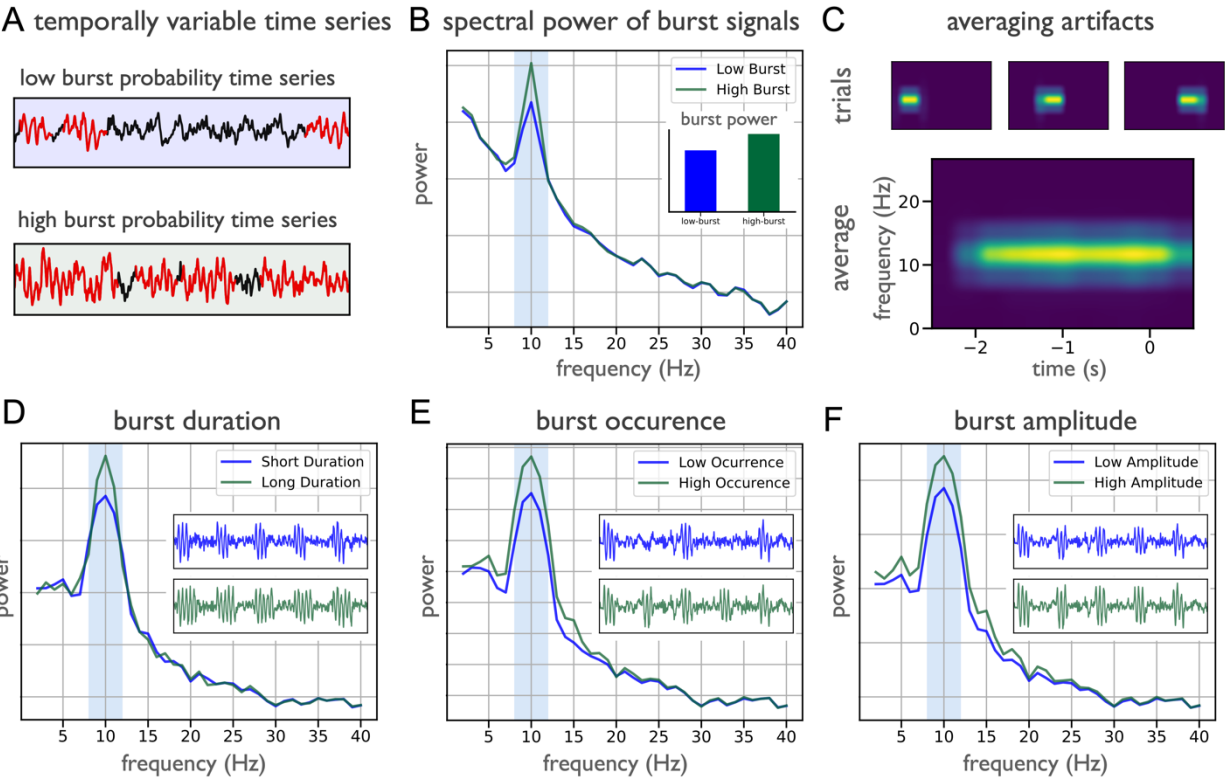
Oscillation Methods

Figure 4: Temporal dynamics of neural oscillations influence spectral measures. A) Two simulated signals with lower (top; blue) and higher (bottom; green) levels of bursting activity in the alpha band, with segments identified as bursts shaded in red. **B**) Power spectra for the signals in A. Note the difference in size of the alpha peak, suggesting a difference in alpha power between the signals. However, when quantifying the power within the bursts (inset bar plot), the power is found to be approximately the same. The apparent difference in power is due to differences in temporal variability. **C**) Temporal variability can lead to spurious sustained power in averaged results. Spectrograms for individual trials (top) show short bursts of oscillatory power, which average to create what appears to be a sustained response (bottom). **D-F**) Measured differences in power can arise due to multiple features of bursting oscillations, including changes in the duration (**D**), occurrence (**E**), and/or amplitude (**F**) of the bursts. Measured power can reflect multiple facets of temporal variability of analyzed time series.
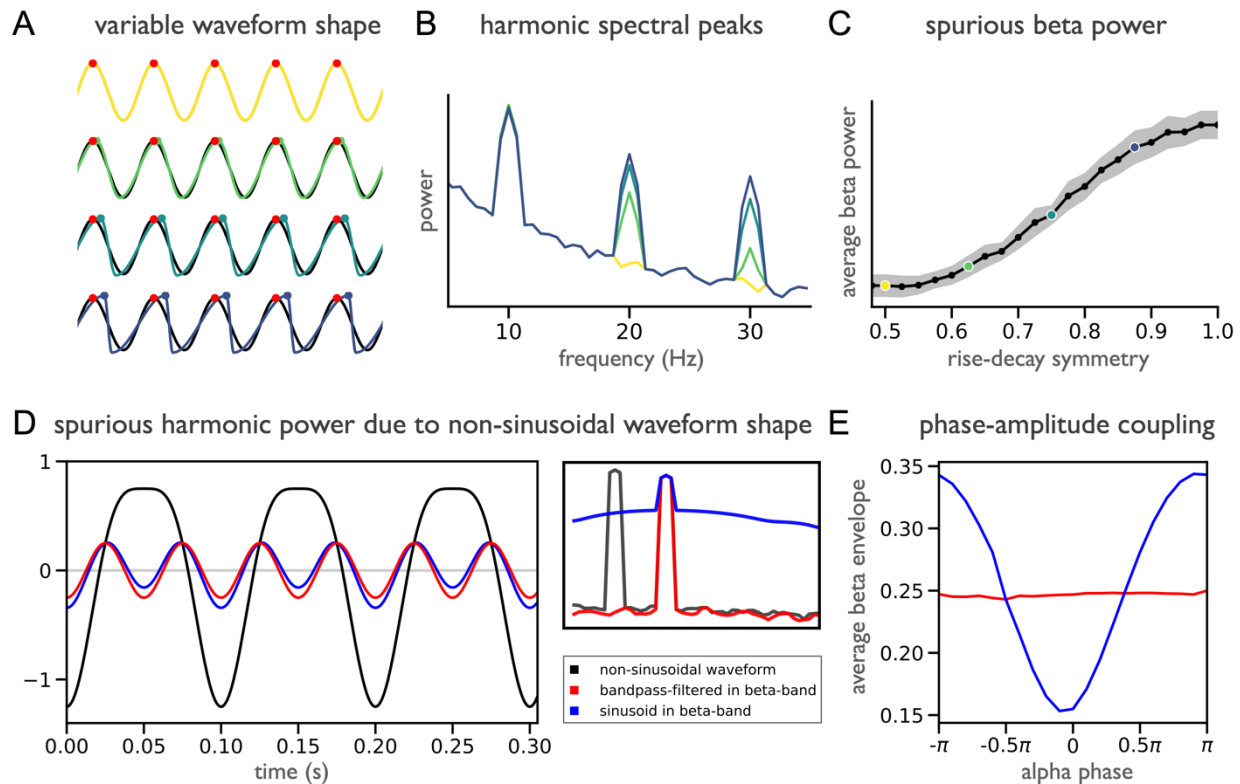
1407

Figure 5: Waveform shape of neural oscillations influences power and coupling measures. A) Four different time domain signals with varying rise-decay asymmetry (colored traces) and their narrowband filtered versions (black traces). Narrowband filtering of asymmetric oscillations shifts the peak times of the signals as indicated by the red dots. **B**) In the corresponding power spectrum, we see emerging spectral peaks at harmonic frequencies (exactly two and three times the frequency) as a result of the asymmetry. **C**) The scale of these harmonic peaks relates to the asymmetry, such that increasing waveform asymmetry can exhibit as increased power in the beta-frequency range. **D**) Non-sinusoidal rhythms can also create spurious phase amplitude coupling. A 10 Hz non-sinusoidal alpha signal is band-pass filtered around the beta peak frequency (17.5 - 22.5 Hz). The beta signal shows deviations in amplitude depending on alpha phase driven by the non-sinusoidal waveform shape (inset shows power spectra for each signal). **E**) Phase amplitude coupling is quantified by calculating beta envelope as a function of alpha phase. In contrast to a pure beta-sinusoid, the beta envelope from the non-sinusoidal signal shows a minimum for a specific alpha phase.
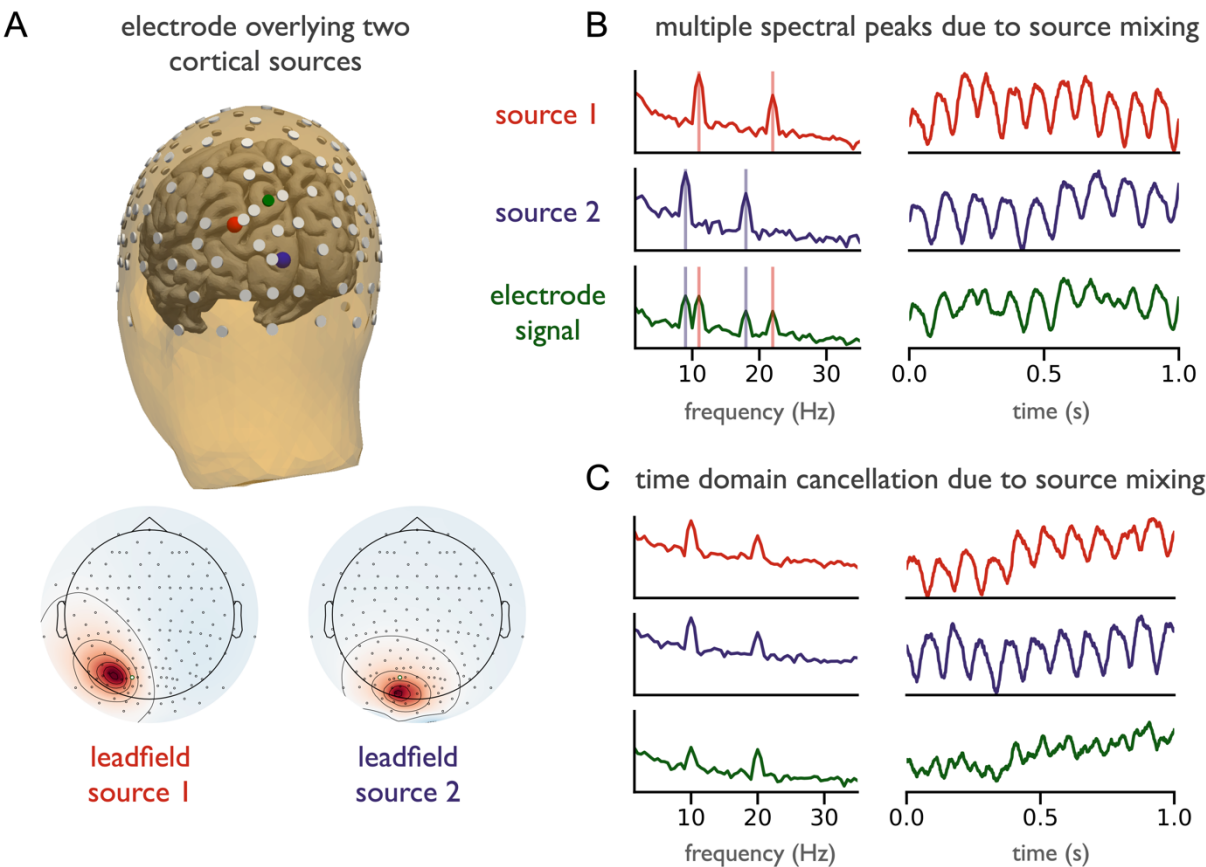
1423

Figure 6: Multiple simultaneous rhythms can interfere and impact sensor level data. A) A realistic
head model with two oscillatory sources (red and blue) placed in the posterior cortex which project on the
highlighted electrode (green). Underneath are the topographies of the two sources that contribute to the
recording electrode. The leadfield coefficients for the two sources have approximately equal values,
indicating equal contribution to the activity recorded at the green electrode. **B**) The simulated electrode
signal (green; bottom) reflects multiple underlying sources, including two distinct rhythmic components, with
slightly different peak frequencies. These sources can be seen as two spectral peaks in the power
spectrum. **C**) Two oscillatory sources with the same peak frequency summate and, due to a phase lag of
pi, do so destructively. In this scenario, interference of the sources cancel each other out at the electrode
level, even though the oscillatory power of the individual sources is stable and consistent.

1424
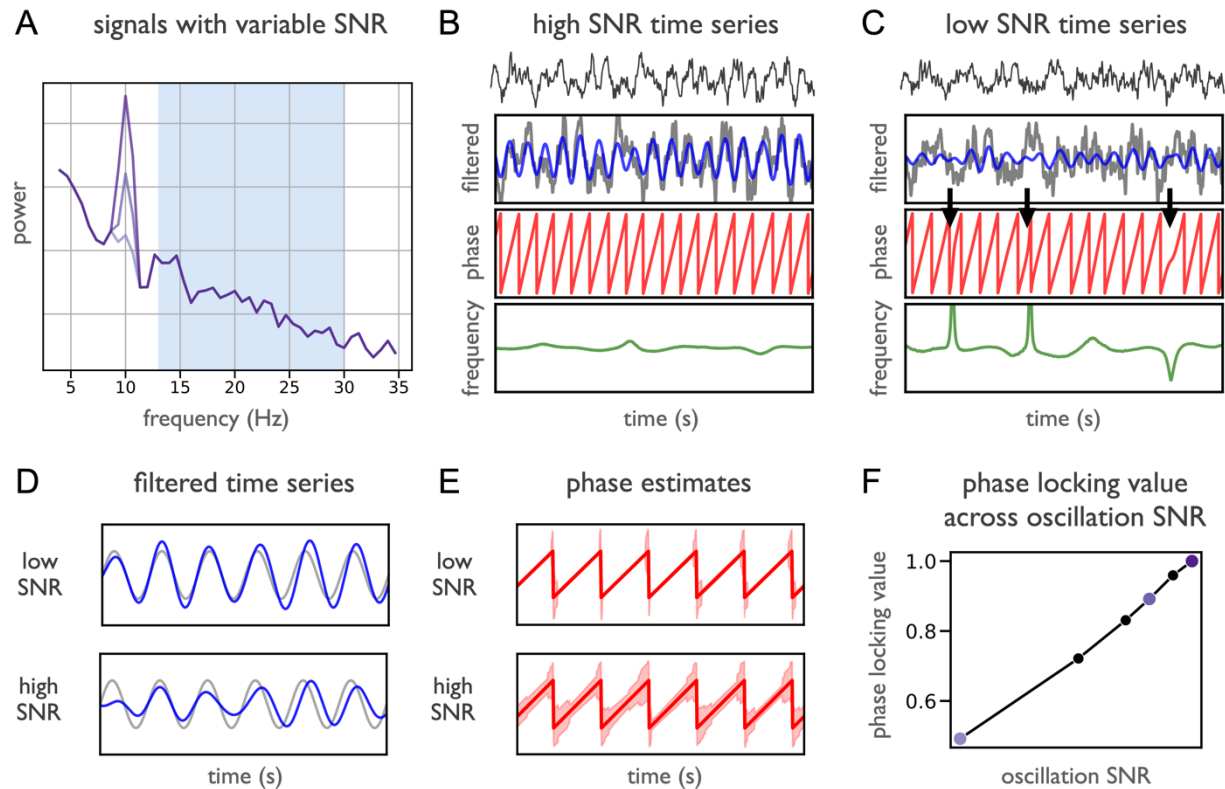1425
1426
1427
1428
1429
1430
1431
1432
1433
1434

1435

Figure 7: Low oscillatory signal-to-noise ratio impacts measures. A) Power spectra for simulated signals with variable SNR for an alpha oscillation, as seen in the different peak heights. **B**) One of the simulated signals, with a high SNR, with the alpha filtered signal (top; blue), from which the instantaneous phase (middle; red) and frequency (bottom; green) are computed. Note that the simulated signal has consistent phase and frequency. **C**) The same as B, for a signal with low SNR. Note that in this case, the estimates of phase and frequency are variable, due to misestimations because of the low SNR. This leads to phase slips, indicated by the arrows, in instantaneous phase, which also leads to erratic estimates of instantaneous frequency. **D**) In the simulated signals, shown with different SNR levels, the underlying signals (grey) are the same, and have uniform phase, however, the filtered traces diverge from the underlying signal. **E**) Phase estimates of the signals in D, in which the solid red is the true phase of the simulated oscillation, and the shading reflects the standard deviation of estimated phase across multiple iterations of phase estimation within each SNR regime. This shows that there is higher variance of phase estimates with lower SNR. These unstable phase estimates will impact subsequent measures, such as phase coupling. **F**) The phase locking value computed between a high powered oscillation, and simulated signals with decreasing power, as shown in A. Note that the simulated oscillations all have the same simulated phase time course, such that there is an expected phase locking value of 1, and any estimates below this are misestimations due to low power.

1453

1454   **Graphical Abstract**

1455

methods for analyzing neural oscillations
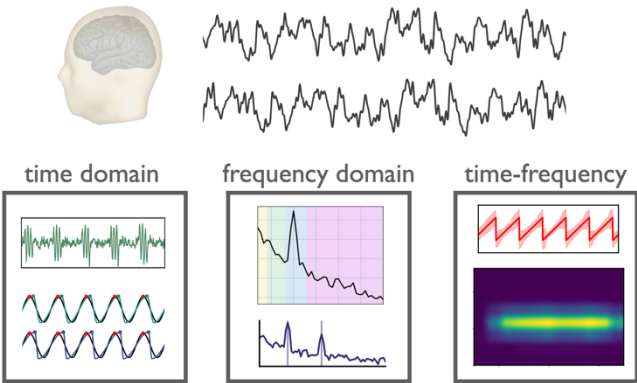
1456

1457   **Graphical Abstract Text**

1458   Neural oscillations are ubiquitous features of neural field data, with great potential for informing

1459   our understanding of neural function and how it relates to cognition. However, there is a great

1460   degree of variability in methods for investigating them, and findings that are reported. In this piece,

1461   we explore methodological considerations for analyzing neural oscillations, that may underlie

1462   some potential misinterpretations, and propose best practice guidelines for addressing them.

1463